Novel Evaluation of Preclinical Models of Peripheral Arterial Disease Using Contrast Enhanced Ultrasound

---

A Dissertation

Presented to

the faculty of the School of Engineering and Applied Science

University of Virginia

---

in partial fulfillment
of the requirements for the degree

Doctor of Philosophy

by

Alyssa B Becker

August 2019

APPROVAL SHEET

This Dissertation
is submitted in partial fulfillment of the requirements
for the degree of
Doctor of Philosophy

Author Signature: 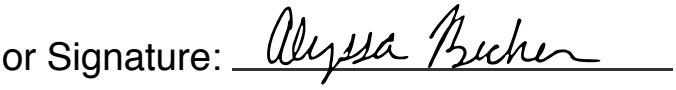

This Dissertation has been read and approved by the examining committee:

Advisor: Brent French

Committee Member: John Hossack

Committee Member: Alexander Klibanov

Committee Member: Silvia Blemker

Committee Member: Will Guilford

Committee Member:

Accepted for the School of Engineering and Applied Science:

Craig H. Benson, School of Engineering and Applied Science

August 2019

Abstract

Peripheral arterial disease (PAD) is a vascular disease resulting from poor perfusion of the extremities, particularly the legs, which affects over 200 million people worldwide. PAD patients incur a similar risk of cardiovascular death as patients with a history of a cardiovascular event. Treatment priority is to reduce risk factors through smoking cessation, diabetes management, etc. as appropriate. One pharmacologic option is cilostazol, which is the only drug approved in the US that has been shown to modestly increase pain-free walking time. Supervised exercise has also been shown to be effective in increasing walking times. There are several additional endovascular and surgical options including: angioplasty, stenting, and bypass procedures. Given the prevalence of PAD, significant economic burden that the disease presents, and the limited efficacy of treatment options, preclinical research to further understand the disease and develop new therapies is critical.

Mouse models are vital in developing new therapeutic approaches to treat PAD. The predominant research method uses a surgical model of hindlimb ischemia (HLI) to cause a reduction in perfusion and laser Doppler perfusion imaging (LDPI) to monitor perfusion over time in the ischemic versus contralateral control limb. Hindlimb ischemia models consist of unilateral ligation(s) or excision of the femoral artery. Despite decades of research and numerous clinical trials, the efficacy of available therapies is still limited. This may suggest shortcomings in current animal models and/or methods of assessment. One promising alternative to LDPI is contrast enhanced ultrasound (CEUS). CEUS uses an intravascular microbubble contrast agent that provides for visualization and

quantification of perfusion. CEUS has been used in several preclinical studies of PAD animal models and has also been applied in the study of patients with PAD. While it has already shown promise, optimization of the technique would increase the utility of the method and its use.

Here, we focus on optimizing CEUS for use in preclinical mouse HLI models. We then assess perfusion measurement methods in a single ligation HLI model of PAD by comparing LDPI (most common technique) and CEUS (emerging technique) with fluorescent microspheres (conventional standard). We also use CEUS to evaluate two more severe surgical models of HLI, a double ligation model and an excision model. In addition, CEUS images are used to assess muscle-specific perfusion patterns resulting from surgery. Finally, we demonstrate how CEUS can be used to evaluate therapies under investigation in a manner that is more relevant to the human disease. We show CEUS is well suited for perfusion measurements in a mouse model of hindlimb ischemia. LDPI measurements show full recovery of perfusion by day 14 post-surgery. In contrast, CEUS shows that perfusion only recovers to ~50% post-surgery. Fluorescent microspheres, histopathology, and photoacoustic microscopy agree with the CEUS findings that perfusion never returns to normal. Similarly, LDPI shows full recovery in both the double ligation surgery and the excision surgery; however, by CEUS there is only ~40% perfusion recovery in the ischemic limb relative to the control limb. Analysis of perfusion post-surgery displays five sets of muscle-specific patterns. Each hindlimb ischemia surgery cohort contained three to five of these groups.

Acknowledgements

First, I would like to thank my advisor, Dr. Brent French, for his guidance over the years. Thank you for always giving me freedom to explore my ideas and providing a wealth of historical context for my work. I would also like to thank my committee members for their contributions. Dr. John Hossack's expertise in ultrasound was vital to the development of the imaging protocol used in this work. Dr. Alexander Klibanov provided the microbubbles used for all experiments, as well as guidance on a variety of chemistry and imaging related topics. Dr. Silvia Blemker provided great advice on experiments and practical advice in navigating research. Dr. William Guilford, for joining my committee on such short notice, and also for teaching me about teaching when I was a TA for his classes. I would additionally like to thank former committee member Dr. Brian Annex for his wealth of clinical and research knowledge in vascular diseases.

I would also like the thank the other members of the French lab. This work would not have been possible without Dr. Lanlin Chen, who performed many surgeries for me and also taught me a lot of experimental techniques. Chris Waters provided help with several experiments and, as the only other graduate student in the lab, was stuck being a sounding board for many things.

Finally, I would like to thank my family and friends who have been a great source of encouragement over the years. A special thank you to Katie, Colleen, Chris, Sunil, and Ana for being both friends and colleagues. You were all there to celebrate successes and, more often, commiserate when experiments weren't working. Thank you to my parents

for their unwavering support and encouragement over the years. Lastly, thank you to Daniel for his love and support, and be a reminder that there is a world outside of lab.

Funding Sources

This work was supported by American Heart Association Grant #15PRE25100003 (Alyssa B. Becker) and NIH/NHLBI grant R01HL116455 (MPI to Brian H. Annex and Brent A. French).

Table of Contents

List of Figures

List of Abbreviations

CAD	Coronary Artery Disease
CEUS	Contrast Enhanced Ultrasound
CLI	Critical Limb Ischemia
CPS	Contrast Pulse Sequence
CUBIC	Clear, Unobstructed Brain/Body Imaging Cocktails and Computational analysis
DSPC	1,2-distearoyl-*sn*-glycero-3-phosphocholine
FGF	Fibroblast Growth Factor
H&E	Hematoxylin and Eosin
HGF	Hepatocyte Growth Factor
HLI	Hindlimb Ischemia
IFA	Iliacofemoral Artery
LA	Alpha Lipoic Acid
LCFA	Lateral Circumflex Femoral Artery
LDPI	Laser Doppler Perfusion Imaging
MB	Microbubble(s)
Micro-CT	Micro Computed Tomography
miRNA	microRNA
MPG	N-(2-mercaptoptopionyl)-glycine
MRI	Magnetic Resonance Imaging
P/SA bifurcation	Popliteal/Saphenous Bifurcation
PAD	Peripheral Arterial Disease

PAM	Photoacoustic Microscopy
PEG	Polyethylene Glycol
PET	Positron Emission Tomography
PET	Pudendoepigastric Trunk
RMSE	Root Mean Squared Error
VEGF	Vascular Endothelial Growth Factor

Chapter 1 : Introduction

Peripheral arterial disease (PAD) is a vascular disease resulting from poor perfusion of the extremities, particularly the legs, which affects over 200 million people worldwide.[1,2] Both arteriosclerosis and microvascular dysfunction have been implicated in the disease process.[3] It is estimated that 12-20% of people over 60 in the US have PAD, and the prevalence is expected to increase as the population ages.[1,4] In the Medicare population, PAD costs over 4.3 billion dollars annually and patients with PAD cost significantly more per year than matched controls.[4,5]

Risk factors of PAD include age, smoking, diabetes, high blood pressure, and dyslipidemia.[6] The classic presentation of PAD is intermittent claudication; claudication is pain, cramping, and tiredness in the legs, especially when exercising (walking, climbing stairs, etc.).[7,8] The presence of these symptoms indicates that a patient should undergo clinical evaluation for PAD. Only 10-15% of patients with PAD have claudication symptoms, with the remaining majority being asymptomatic, leading to a large undiagnosed and untreated population.[6] PAD patients incur a similar risk of cardiovascular death as patients with a history of a cardiovascular event.[9] In patients with PAD the mortality due to coronary artery disease (CAD) and all-cause mortality are 6.6 and 3.1 fold higher, respectively, than that of a person without PAD.[9]

In addition to the increased risk of death, PAD can play a significant role in quality of life as patients progress through some or all of the stages of the disease. These stages are asymptomatic PAD, claudication, pain at rest, and eventually gangrene (death of tissue).[6]

Severe PAD or critical limb ischemia (CLI), often confounded by other comorbidities, can result in gangrene and require amputation of the affected portion of the limb.[6,10] For cases that are diagnosed before requiring amputation, several treatment options aim to reduce cardiovascular risk and to reduce symptoms. Treatment priority is to reduce risk factors through smoking cessation, diabetes management, etc. as appropriate.[6,10] One pharmacologic option is cilostazol, which is the only drug approved in the US that has been shown to modestly increase pain-free walking time.[7] Cilostazol has both vasodilatory and antiplatelet effects, both mediated through endothelial cells.[11] Vasodilation likely occurs through a nitric oxide dependent mechanism and reduced platelet activation and aggregation occurs through the inhibition of phosphodiesterase III.[11] Supervised exercise has also been shown to be effective in increasing walking times.[7] When PAD symptoms are significantly affecting quality of life there are also several endovascular and surgical options including: angioplasty, stenting, and bypass procedures.[6,10,12] These interventions are generally initially successful but vessel patency can significantly decrease within five years depending on the procedure, location, and severity of the disease.[13]

Given the prevalence of PAD, significant economic burden that the disease presents, and the limited efficacy of treatment options, preclinical research to further understand the disease and develop new therapies is critical. The majority of PAD research is done with mouse models of the disease. Rabbit and pig models are also suitable, though the increased expense and limited availability of transgenic models limits their use for many studies.[14] Despite decades of research and many clinical trials there are few effective

therapies.[15] This suggests that our animal models and/or methods of assessment may be inadequate.

The predominant research method uses a surgical model of hindlimb ischemia (HLI) to cause a reduction in perfusion and laser Doppler perfusion imaging (LDPI) to then monitor perfusion over time in the ischemic versus contralateral control limbs. Hindlimb ischemia models consist of unilateral ligation(s) of the femoral artery, some models also excise the artery. Depending on the number and location of these ligations, and other factors including environment and strain of mouse, the extent of tissue necrosis and the degree of the evoked angiogenic response can vary.[16–19] Depending on these and other variables, LDPI typically indicates that blood flow to the ischemic limb is fully restored within two weeks of HLI surgery: a phenomenon referred to as “perfusion recovery”. In HLI models, LDPI measures perfusion in the feet as a ratio of the ischemic to control limb. While LDPI is common and easy to use, it is inherently limited as an optical technique because it only measures perfusion at superficial levels of tissue (<700 μm).[20] Another limitation of LDPI is that measurements are taken in the feet, whereas biochemical, histochemical and functional studies of HLI typically interrogate the calf muscles. Because LDPI is so widely used as the primary endpoint for HLI studies, it is conceivable that these limitations might play a determining role in the success of translating preclinical findings into effective clinical therapies. A critical evaluation of independent techniques for measuring perfusion in HLI models may thus reveal novel findings and suggest new avenues of investigation.

Imaging techniques are well suited to characterize perfusion, and one promising alternative to LDPI is contrast enhanced ultrasound (CEUS).[21] CEUS uses an intravascular microbubble contrast agent that provides for visualization and quantification of perfusion and is especially suited for serial measurements.[21] This technique has the additional advantage of being able to image a cross-section of the entire calf, potentially providing muscle-specific perfusion information. CEUS has been used in several preclinical studies of PAD animal models and has also been applied in the study of patients with PAD.[22–27] While it has already shown promise, optimization of the technique would increase the utility of the method and its widespread use.

In addition to improving preclinical perfusion measurement techniques, animal models themselves can be further evaluated. Anatomic variations in vasculature structure can cause HLI surgery to produce different results in one individual versus another.[28,29] While LDPI is not able to interrogate calf muscle perfusion, CEUS will be able to provide new insight into how individual muscles respond after undergoing HLI. Investigating this variation in individual muscle perfusion has strong potential to improve current surgical models, thus enabling future advances in PAD research.

In this dissertation, we implement and refine CEUS imaging and test the hypothesis that CEUS can measure perfusion in mouse HLI models. We measure perfusion in an HLI model by LDPI and CEUS, then compare the results to the gold standard fluorescent microsphere measurements. Furthermore, we apply microbubble perfusion measurement methods to interrogate and improve surgical mouse models of hindlimb ischemia and

study perfusion recovery in these models. Towards this end, we evaluate existing and new surgical models of hindlimb ischemia to identify optimal excision/ligation combination(s) to explore the dynamic range of pathology. We investigate muscle-specific perfusion responses in different HLI models. We also investigate individual variations of muscle perfusion from mouse to mouse subjected to the same HLI surgery. Finally, we use an optimized mouse model of PAD and CEUS imaging to evaluate the potential of two potent antioxidants for the treatment of PAD.

Chapter 2 : Contrast Enhanced Ultrasound Reveals Partial Perfusion Recovery after Hindlimb Ischemia as Opposed to Full Recovery by Laser Doppler Perfusion Imaging

Introduction

Peripheral arterial disease (PAD) is caused by obstructions to blood flow in the legs due to atherosclerosis.[30] PAD affects over 200 million people worldwide and has very limited treatment options.[1] Many therapeutic approaches fail in clinical trials, suggesting that preclinical models and assessment methods may be imperfect.[15,31]

Mouse models of PAD are widely used and typically consist of a unilateral ligation(s) of the femoral artery to induce hindlimb ischemia (HLI).[31] There are a variety of perfusion measurement techniques that can be applied to HLI models. Fluorescent (or radioactive) microspheres are the conventional standard for regional perfusion measurements. Microspheres are injected into arterial circulation and lodge in the capillaries in proportion to perfusion. They can be quantified ratiometrically or absolutely, under certain conditions.[32] Microspheres are commonly used in large animal studies, however very few groups use them in mice because of the low flow velocities and small blood volumes in mouse skeletal muscle.[33] The microsphere technique is also destructive, making serial studies more difficult and thus leading to the use of alternative methods by most groups using HLI models.

Laser Doppler perfusion imaging (LDPI) is the most commonly used technique to evaluate perfusion recovery after HLI. LDPI is an optical technique using the principle of laser speckle contrast analysis where a laser trained on a region creates a speckle pattern caused by interference from moving particles.[34,35] It is simple to use and outputs a heat map of perfusion in the area of interest, which is typically the feet in most mouse models of HLI. Based on the physics of the measurement, this technique is only valid as a relative measure of perfusion as a ratio between different areas within the same image frame.[36] A limitation of LDPI is that measurements are typically made in the feet, whereas biochemical, histochemical and functional studies of HLI typically interrogate the muscles in the leg. Since LDPI is an optical technique, an inherent constraint is the limited depth of tissue that can be interrogated (~700 μm).[20,37]

A promising alternative technique for perfusion measurements in HLI models is contrast enhanced ultrasound (CEUS). CEUS is a well-established technique for assessing perfusion and has been applied clinically for coronary artery disease, peripheral arterial disease, and cancer applications, as well as preclinically for kidney, adipose, heart, and tumor perfusion measurements.[38,27,25,39–43] The contrast agent is a microbubble with a lipid shell and gas core that is purely intravascular. Microbubbles are best visualized in a nonlinear (harmonic) contrast mode that is available on many clinical scanners which allows the microbubble signal to be distinguished from the tissue signal. CEUS is well suited for perfusion measurements in skeletal muscle, and a few groups have utilized the technique, but it has yet to be thoroughly explored or widely implemented.[23,44–46] CEUS

has the potential to overcome several of the limitations of LDPI, as well as add the resolution needed to evaluate perfusion on a per muscle basis.

Here we test the hypothesis that CEUS can be used to serially assess perfusion recovery in a mouse HLI model of PAD. We measured perfusion recovery over time by LDPI and CEUS, then compared the results to traditional microsphere measurements.

Background

LDPI

Laser Doppler perfusion imaging uses the principle of laser speckle contrast analysis to measure an index of perfusion.[47] A laser is trained on a user-determined area of interest and there is a resulting 2-D speckle pattern based on the scattering of light off of the medium.[34,47] Decorrelation of the speckle pattern indicates movement in the area being quantified.[34] The output is a heat map in arbitrary perfusion units and results are reported as a ratio of two regions of the image.[47] LDPI is unable to provide absolute measurements due to an unknown incident angle, underlying vascular structure, and influence of multiple scattering.[34,48] When utilizing LDPI to measure perfusion in mouse HLI models, the feet are typically the region of interest. The ischemic limb is normalized to the control limb and perfusion recovery is reported as a ratio or percentage. The use of LDPI to assess HLI models presents a number of limitations. Given that LDPI is an optical technique, signal can only be measured up to about 700 μm deep.[20] The measurement in also biased towards more shallow structures, with the vasculature at depths <300 μm causing more scattering and thus more signal.[20] Since the assessment of HLI is done without opening

the skin, most of the signal is arising from the skin (~450 μm thick) itself, rather than underlying muscle vasculature.[49,50] Another limitation is that the assessment of perfusion is typically done in the feet rather than in the calves. Both clinically and preclinically most other assessments, such as angiography or histology, are done in the muscles of the calves or thighs where PAD primarily manifests.[51,52] Further discussion and assessment of why the feet are used in HLI models is presented later in this chapter.

CEUS

Contrast enhanced ultrasound (CEUS) uses a microbubble as the contrast agent, which generally consists of a lipid or protein shell and a gas core. Microbubbles are typically 1-10 μm in diameter and purely intravascular. Microbubbles are visualized in a specific contrast mode which is present on many ultrasound scanners. These contrast agents oscillate when ultrasound is applied, causing the generation of an acoustic signal in the fundamental frequency and at nonlinear harmonic frequencies.[53,54] These nonlinear signals allow the microbubbles to be distinguished from tissue. At steady state, high power (mechanical index) burst pulses can be applied that causes the microbubbles in the field of view to burst; microbubbles from upstream continue to flow into the scanning plane, thus enabling perfusion to be quantified.[22] Quantification is typically performed using Equation 1. In this equation A is the image intensity and represents blood volume, β represents blood velocity and A*β is the slope after the burst pulse and represents blood flow.[22] The form of this equation can be derived from a single compartment model assuming a well mixed system, constant volume, constant flow, constant rate of infusion,

(1)

no reacting species, impermeable wall, as well as that the sum of individual vessels can be modeled as a single inlet and outlet (Appendix A).

$$\boldsymbol{y = A(1 - e^{-\beta t})}$$

Materials and Methods

Mice

C57BL/6 male mice were purchased from Jackson Laboratory (Bar Harbor, ME, USA). Mice were provided standard chow and water *ad libitum*. They were housed 1-4 per cage in a room with a 12 hour light cycle. Cages contained corn cob bedding except during surgical recovery where iso pad bedding (Envigo, City, State, USA) was used until mice were ambulating normally. The Institutional Animal Care and Use Committee of the University of Virginia approved all animal experiments.

Mouse Model of Hindlimb Ischemia

10-12 week old mice were anesthetized with ketamine (90mg/kg) and xylazine (10 mg/kg). The left medial leg was shaved, depilated, and the area was prepared for aseptic surgery. Mice were kept under a heating lamp to maintain body temperature. An incision was made in the thigh to expose the femoral artery. 6-0 silk sutures were used to ligate the femoral artery proximal to the lateral circumflex femoral artery **(Figure 2-1**).[28] Care was taken to not damage major nerves or veins. Buprenorphine-SR (0.5 mg/kg) was administered after surgery and as needed in subsequent days.

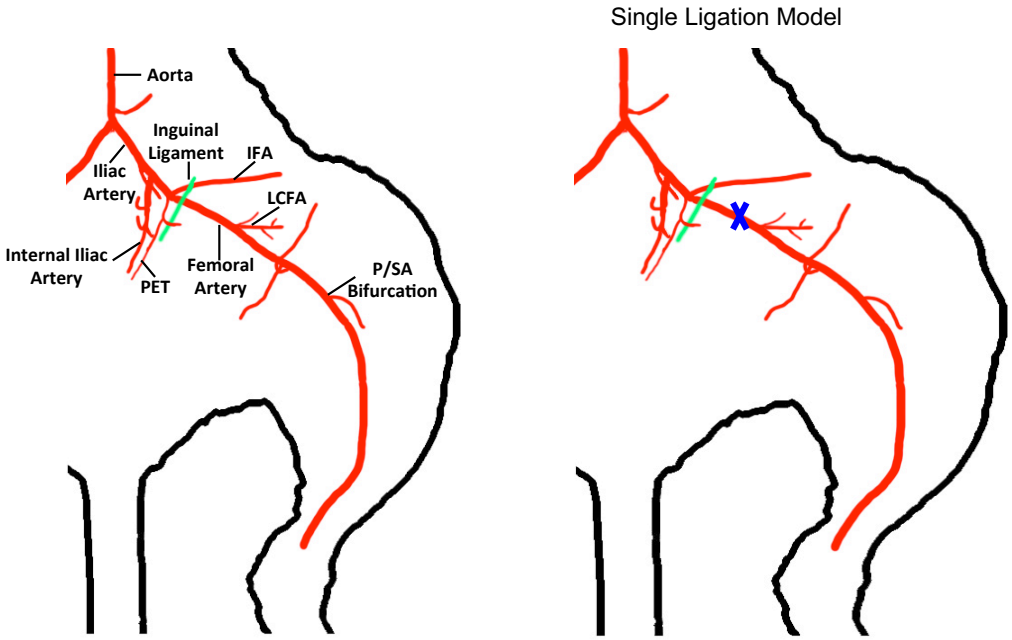

Adapted from Kochi, Takashi, et al. PloS one, 8.12 (2013): e84047.

Figure 2-1 Single Ligation HLI Model

The arterial anatomy of the mouse hindlimb. The single ligation model of HLI with the "X" showing the location of the ligation above the lateral circumflex femoral artery (LCFA).

Laser Doppler Perfusion Imaging (LDPI)

Mice were anesthetized with 1-2% isoflurane and calves were shaved and depilated. Mice were placed prone under the LDPI instrument (Perimed, Sweden), legs extended, and feet secured in place. Three to five measurements were taken, about one minute apart. Data were analyzed using the included PimSoft analysis software. ROIs were selected around the feet, the image intensity was averaged over all measurements, and a ratio of left:right (ischemic:control) foot was calculated.

Microbubble (MB) Preparation

Microbubbles were prepared from decafluorobutane gas, which was dispersed in normal saline by sonication, essentially as described earlier.[55] Microbubbles were stabilized with a lipid monolayer shell that consisted of 1,2-distearoyl-*sn*-glycero-3-phosphocholine (DSPC) and PEG stearate. The presence of microbubbles greater than 7 μm was minimized by flotation at normal gravity, to ensure none get trapped in the lungs. The vial concentration was measured approximately every two weeks using a Coulter Counter (Beckman Coulter, Indianapolis, Indiana, USA). If needed, the microbubbles were diluted with sterile saline just before use.

Contrast Enhanced Ultrasound (CEUS)

Imaging was performed with an Acuson Sequoia C512 system and a 15L8W transducer (Siemens, Munich, Germany). Mice were anesthetized with 1-2% isoflurane in air. A catheter with a 27G needle at the end was filled with heparinized saline (100 units/ml),

inserted in the tail vein and secured. Mice were placed prone on a heated stage, legs extended, and feet secured. Ultrasound gel was placed on the calves and the transducer was positioned mid-calf, taking care to maintain the same focal length each time. Scanning parameters were optimized and held constant as follows: frequency was 7 MHz, dynamic range was 100 dB, gain was -10 dB, imaging mechanical index was 0.2, burst mechanical index was 1.9, and burst time was one second. Video of the ultrasound exam was acquired in real time. Several B-mode frames were acquired before switching to contrast imaging mode. Microbubble solution was infused through the tail vein catheter at $1x10^7$ MB/min. During imaging, the syringe was rotated approximately every 30 seconds to prevent the microbubbles from floating and changing the concentration being infused. After steady state was reached, about 5 minutes after the start of the infusion, high mechanical index burst pulses were applied once per minute for 10-15 minutes. The high mechanical index pulses cause the microbubbles in the field of view to burst; microbubbles from upstream continue to flow into the scanning plane, thus enabling perfusion to be quantified.[22]

Video data were analyzed using a custom MATLAB (Mathworks, Natick, Massachusetts, USA) script. B-mode images were segmented with a combination of morphological operations, circular Hough transform, and active contouring to define ROIs for the left and right limbs. Segmentation was manually checked to ensure the resulting ROIs were not biased by image artifacts. Several parameters could be modified to remove artifacts as needed to allow proper segmentation by the program. Image intensity over time was calculated and each flash-replenishment sequence was separated to allow for curve fitting. The first value after the high mechanical index pulse was taken as the background

and subtracted out for each individual sequence. The data were fit to $y=A(1-e^{-\beta t})$ where A represents blood volume, β represents blood velocity and $A^*\beta$ represents blood flow.[22] After excluding any sequences with obvious aberrations, the four sequences with the lowest RMSE were averaged to calculate $A^*\beta$ at each timepoint. The average left:right (ischemic:control) $A^*\beta$ ratio was calculated for direct comparison with LDPI.

Fluorescent Microspheres

Microspheres were sonicated no more than 24 hours prior to administration and were vortexed immediately before administration. Mice were anesthetized with pentobarbital (75 mg/kg) and intubated at 100 breaths/minute. The chest was opened and 200,000 green fluorescent microspheres (15 μm in diameter, Invitrogen, Carlsbad, California, USA) were injected into the left ventricle over two minutes.[56] The microspheres were allowed to circulate for five minutes. Skeletal muscle on both limbs from just below the knee to just above the ankle was harvested and the bones were removed. Both kidneys were also harvested for reference purposes. Each tissue was blotted dry, weighed, and placed in a vial with a known amount of liquid and homogenized with a handheld, electric tissue homogenizer. Samples of homogenate from each tissue piece were placed on slides and sealed with a coverslip. The number of microspheres were counted on a fluorescence microscope (Olympus BX41, Olympus, Tokyo, Japan) and converted into units of spheres/g tissue to standardize a ratio of the left to right limb (ischemic:control) for comparison with LDPI and CEUS. Mice were excluded if there were less than 400 microspheres in the control limb, or if the kidneys were >15% different, indicating incomplete blood pool mixing.[23,32,57,58]

Tissue Clearing and Microscopy of in situ Fluorescent Microspheres

Muscle containing fluorescent microspheres was incubated in 4% paraformaldehyde at 4˚C for 48-72 hours then rinsed three times with saline. A previously described CUBIC protocol was used for tissue clearing.[59] Incubation time was reduced as skeletal muscle clears significantly in just three days. Thin sections of muscle were teased apart, placed on slides, and sealed with a cover slip. Images were acquired on a fluorescence microscope (Olympus BX41, Olympus, Tokyo, Japan).

Histological Analysis

Mice were anesthetized with ketamine (90mg/kg) and xylazine (10 mg/kg), the chest was opened, and mice were perfused with heparinized saline (10 units/ml) followed by 4% paraformaldehyde. Skeletal muscles were harvested and incubated in paraformaldehyde at 4˚C for 48-72 hours. Tissue was rinsed three times in saline and submerged in 15% sucrose overnight and then 30% sucrose overnight before flash freezing in OCT. 10 μm sections were cut and stained with hematoxylin and eosin (H&E).

Photoacoustic Microscopy (PAM)

Mice were anesthetized with 1-2% isoflurane and placed prone on a heated stage, legs extended, and feet secured. An incision was made in the skin along the gastrocnemius and the skin was secured so the muscle remained visible. Photoacoustic microscopy was performed as previously described.[60]

Statistical Analysis

All results are presented as mean±SEM. A linear mixed model with Bonferroni correction was used to analyze the longitudinal LDPI and CEUS data using SAS version 9.4 (SAS Institute, Inc., Cary, NC, USA). Comparisons between more than two groups were performed with a one-way ANOVA and post-hoc analysis (Tukey's test) as appropriate. $P<0.05$ was considered significant. Except as noted, GraphPad Prism version 5.0 (GraphPad Software, San Diego, CA, USA) was used to perform statistical analyses.

Results

CEUS is Well Suited for Hindlimb Perfusion Assessments

The optimal transducer position for imaging the hindlimbs allowed the imaging plane to assess both calves simultaneously (**Figure 2-2**). Imaging and microbubble infusion parameters were optimized for this application. With these optimized parameters, imaging was performed at the upper limit of the linear range ($1x10^7$ MB/min) (**Figure 2-3**). To evaluate variability within and between mice, four normal mice were assessed at four different time points with CEUS (**Figure 2-4**). As anticipated, normal mice exhibited modest variability in left:right perfusion ratios over time, comparable with human subject variability.[61,62] Repeated perfusion measurements taken during a single imaging session exhibited minimal variability (**Figure 2-5**).

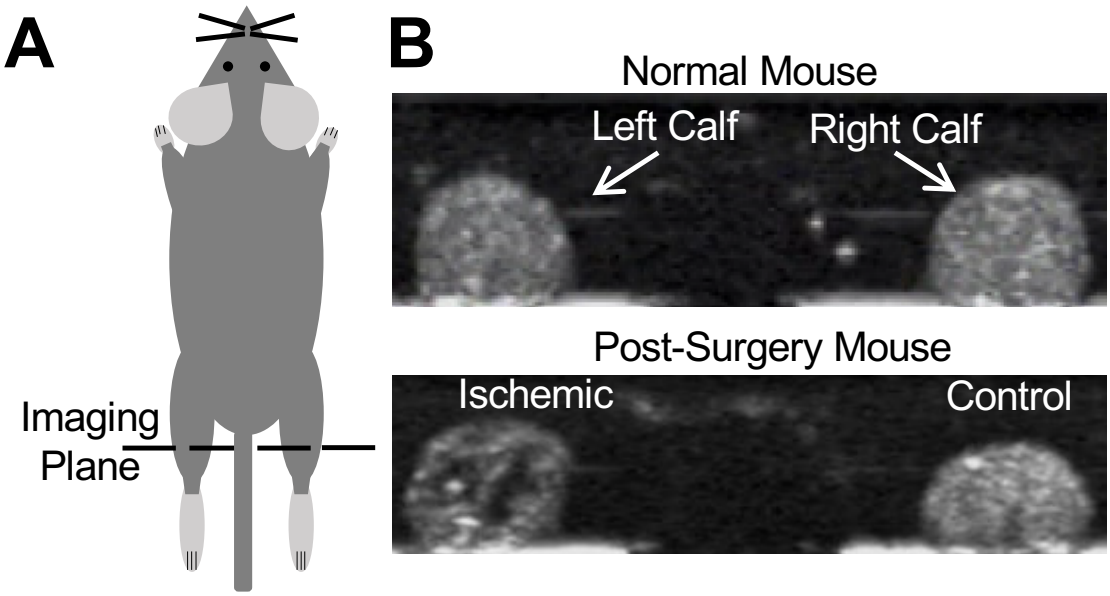

Figure 2-2 CEUS Imaging Setup

A) Schematic of the transducer placement across both calves. B) Example CEUS images of calf cross sections in contrast mode with microbubbles in circulation in a normal mouse and a mouse that underwent HLI surgery. The ischemic limb in the post-surgery mouse has a lower image intensity and areas with minimal flow.

A

Variable	Range Tested	Optimized Value
Frequency	7-12 MHz	7 MHz
Dynamic Range	55-100 dB	100 dB
Gain	-20-0	-10
Flash Replenishment Interval	20-60 s	60 s
Burst Time	1-2 s	1 s
MB Concentration	$1x10^8$-$1x10^9$ MB/ml	$1x10^9$ MB/ml
MB Infusion Rate	2.5-20 μl/min	10 μl/min

B

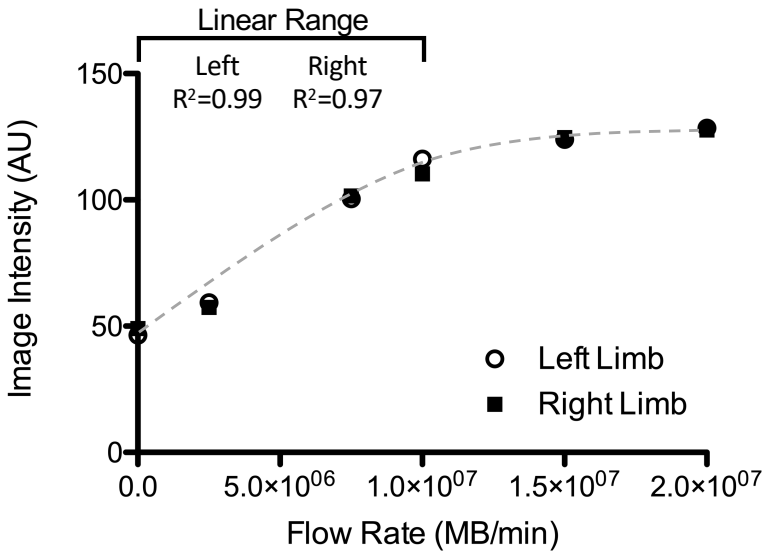

Figure 2-3 CEUS Optimized Imaging Parameters

A) Tested and optimized values for relevant ultrasound parameters. B) Image intensity in the left and right limbs of one mouse over a range of concentrations with the linear range up to $1x10^7$ MB/min.

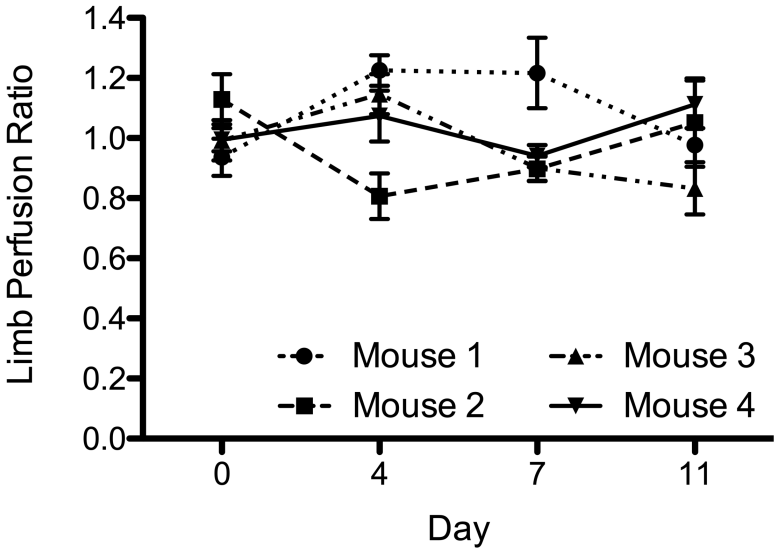

Figure 2-4 CEUS Between Mice Variability

Test-retest measurements of hindlimb blood perfusion ratios by CEUS in four mice each measured four times over eleven days shows modest variation over time. Measurements during a single imaging session showed minimal variation.

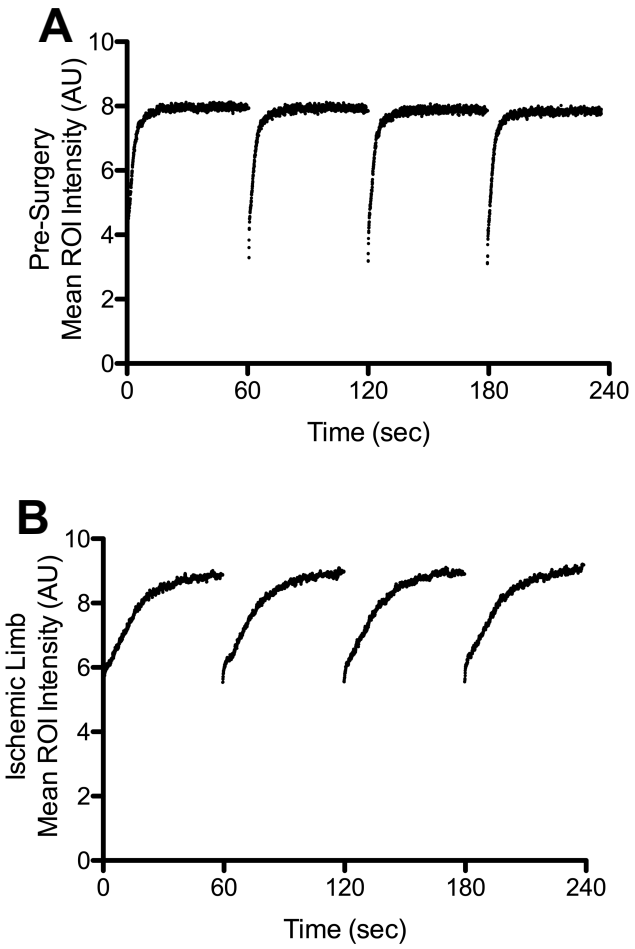

Figure 2-5 CEUS Within Mouse Variability

A) Example of four sequences of flash-replenishment data from a single normal limb. B) Example of four sequences of flash-replenishment data from a single limb one day post-surgery showing a much slower rate of microbubble replenishment (intensity increase), indicating lower perfusion.

CEUS and LDPI Show Different Perfusion Recoveries Over Time

To compare perfusion recovery as measured by LDPI and CEUS, mice were imaged by both techniques before surgery and days 1, 4, 7, 14, 28, 60, 90, and 150 after surgery (**Figure 2-6**, **Figure 2-7**). Perfusion ratios by LDPI and CEUS were significantly different at every time point except day 4 post-surgery. Day one post-surgery, perfusion in the ischemic limb as measured by LDPI was reduced to 72% of the control limb. Perfusion in the ischemic limb then increased until day 14 post-surgery, at which time it returned to pre-surgery levels and remained steady until day 150 post-surgery. By CEUS, day one post-surgery perfusion in the ischemic limb was reduced to 25% of the control limb. In contrast to LDPI, perfusion by CEUS increased until day 4 post-surgery when it reached a peak of 77% of the control limb and remained similar at day 7 post-surgery at 69% of the control limb. A modest decline was noted by CEUS from day 7 to day 14 post-surgery, but perfusion in the ischemic limb leveled off to an average of 56% of the control limb for the duration of the study (until 150 days post-surgery). Since there were small differences between LDPI and CEUS perfusion ratios before surgery, the data were also analyzed as a change from the pre-surgery perfusion ratios. By LDPI, perfusion returned to normal by day 28 post-surgery; but by CEUS, perfusion in the ischemic limb never returned to normal.

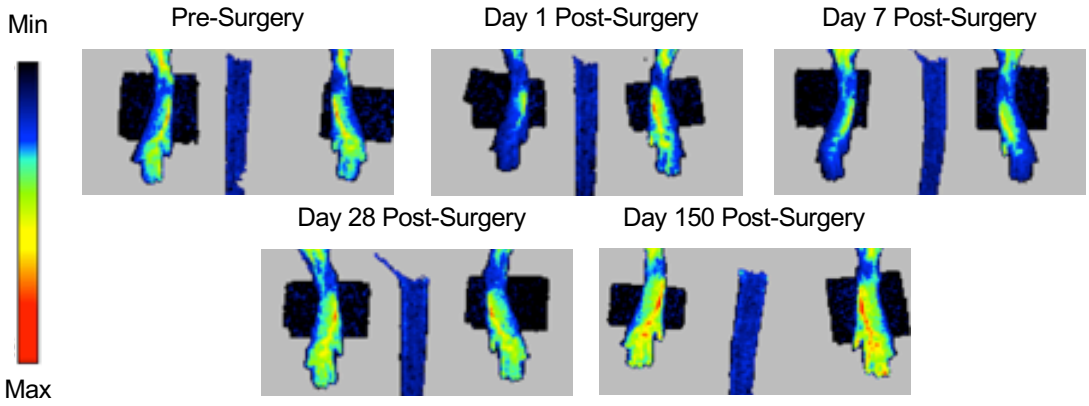

Figure 2-6 LDPI Perfusion Recovery After Single Ligation HLI

Representative images of perfusion recovery measured by LDPI before surgery and days 1, 7, 28, and 150 post-surgery. The ischemic limb is on the left in each image.

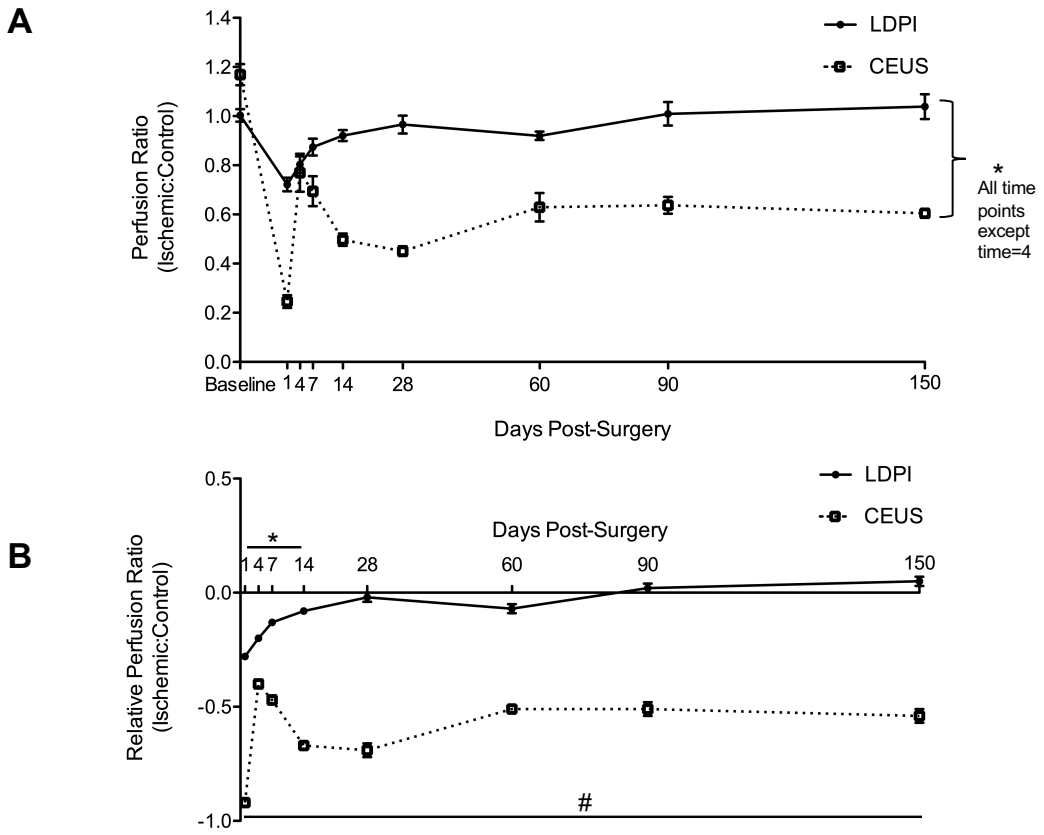

Figure 2-7 CEUS Perfusion Recovery After Single Ligation HLI

A) The ratio of perfusion in ischemic:control limbs as measured by LDPI and CEUS at baseline and days 1, 4, 7, 14, 28, 60, 90, and 150 after surgery. By LDPI, perfusion returns to normal within 14 days post-surgery. However, by CEUS perfusion is more severely reduced at day 1, then improves modestly at days 4 and 7 before achieving a plateau at ~50% of the control limb through the end of the study. Measurements by LDPI and CEUS are significantly different at all time points except day 4 post-surgery (*$p<0.05$; n=17 for pre-14 day time points, n=7 for 28-150 day time points). B) The ratio of perfusion in ischemic:control limbs relative to the pre-surgery perfusion ratios. By LDPI, perfusion returns to normal by day 28 post-surgery (*$p<0.05$) , but by CEUS perfusion never returns to normal (#$p<0.001$). Statistical analysis was performed using a linear mixed model with Bonferroni correction.

LDPI Perfusion Recovery in the Foot Versus Calf

Since LDPI measurements are more typical in the foot, we chose to use those measurements to compare with CEUS. However, given the difference in the CEUS and LDPI results, measurements in the calves by LDPI were performed before surgery and days 1, 4, 7, and 14 after surgery (**Figure 2-8**). Before surgery, the perfusion ratio in the calves was 1.09 vs 1.01 in the feet. Day one post-surgery, perfusion in the ischemic calf was greater than in the foot, 0.85 vs 0.72. Perfusion recovery was faster in the calves than the feet, corresponding to the lesser initial reduction in perfusion.

Fluorescent Microspheres Show Impaired Perfusion

As the results from LDPI and CEUS differed significantly, relative perfusion between limbs was additionally assessed by fluorescent microspheres, the conventional standard for perfusion measurements. Perfusion by LDPI, CEUS, and fluorescent microspheres were compared at day 14 post-surgery (**Figure 2-9**). LDPI showed a normal perfusion ratio (0.9 ± 0.1) which was significantly different than both CEUS (0.5 ± 0.1) and fluorescent microspheres (0.6 ± 0.2). CEUS and fluorescent microspheres were not significantly different, both demonstrating that perfusion never returns to normal in mice subjected to hindlimb ischemia.

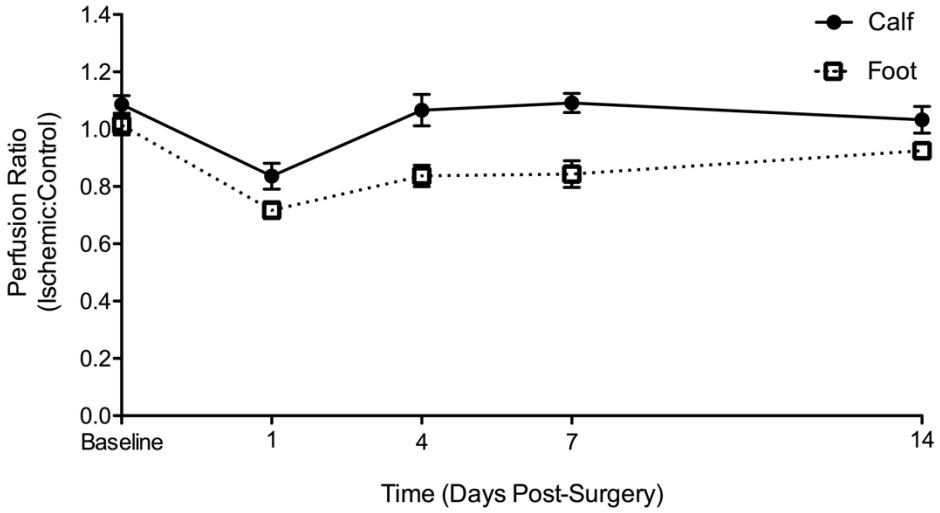

Figure 2-8 LDPI Perfusion Recovery in the Foot Versus Calf

Perfusion recovery measured by LDPI in the feet and calves before surgery and days 1, 4, 7, and 14 post-surgery. The calf has a slightly higher perfusion ratio before surgery, 1.09±0.03 vs 1.01±0.03 in the feet. Day one post-surgery, perfusion in the ischemic calf was greater than in the foot, 0.85±0.05 vs 0.72±0.03. Corresponding to this lesser initial reduction in perfusion, perfusion recovery was faster in the calves than the feet.

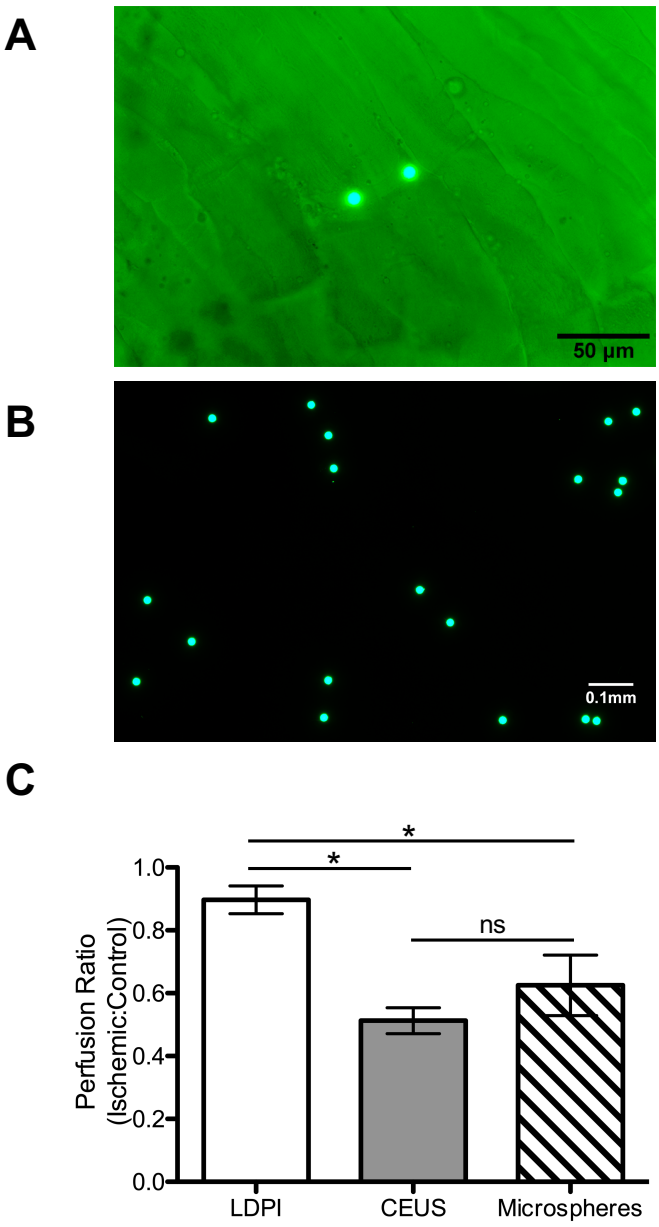

Figure 2-9 Fluorescent Microsphere Measurement of Perfusion

A) Green fluorescent microspheres in mouse skeletal muscle, imaged at 200x B) Green fluorescent microspheres, imaged at 100x. C) Comparison of perfusion ratios measured by LDPI, CEUS, and fluorescent microspheres day 14 post-surgery. CEUS and fluorescent microspheres show good agreement with 50-60% perfusion recovery, while LDPI shows nearly complete recovery (n=5, *p<0.05) Statistical analysis was performed with a one-way ANOVA and Tukey's test for post-hoc analysis.

Pathological Muscle Morphology and Function

Muscle morphology in control and ischemic limbs was evaluated with H&E staining day 150 post-surgery (**Figure 2-10**). Muscle from the ischemic limbs showed irregular fibers and many fibers with centralized nuclei. In control limbs, the majority of muscle fibers have peripheral nuclei and there is a more consistent fiber architecture. Photoacoustic microscopy was used to evaluate oxygen saturation, perfusion, and vascular structure before HLI and 14 days post-surgery in gastrocnemius muscle (**Figure 2-11**). Results indicated that oxygen saturation and perfusion remain reduced 14 days post-surgery, consistent with recent reports.[63] Anatomically, the vasculature was irregular and tortuous, and there were very few larger vessels evident.

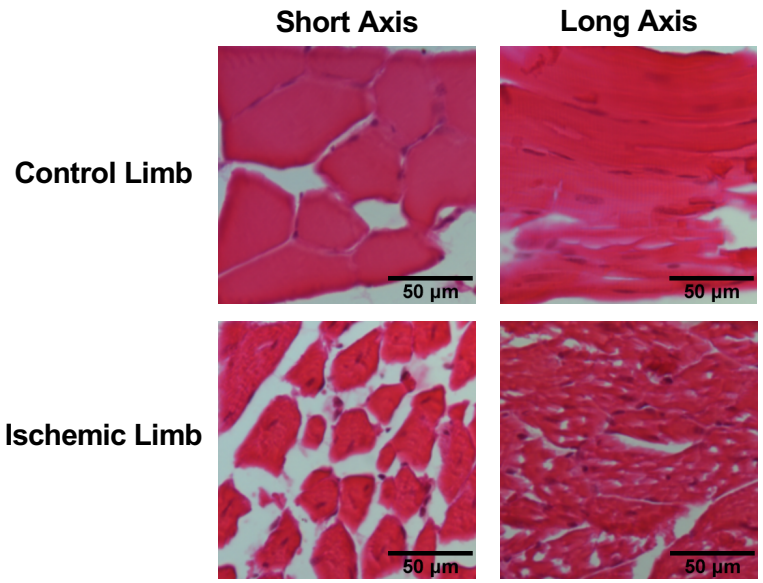

Figure 2-10 Muscle Morphology After Single Ligation Surgery

H&E staining of muscle 150 days post-surgery at 200x. Representative control limb muscle shows peripheral nuclei and uniform myofiber architecture. Representative ischemic limb muscle shows irregular myofibers and many myofibers with centralized nuclei.

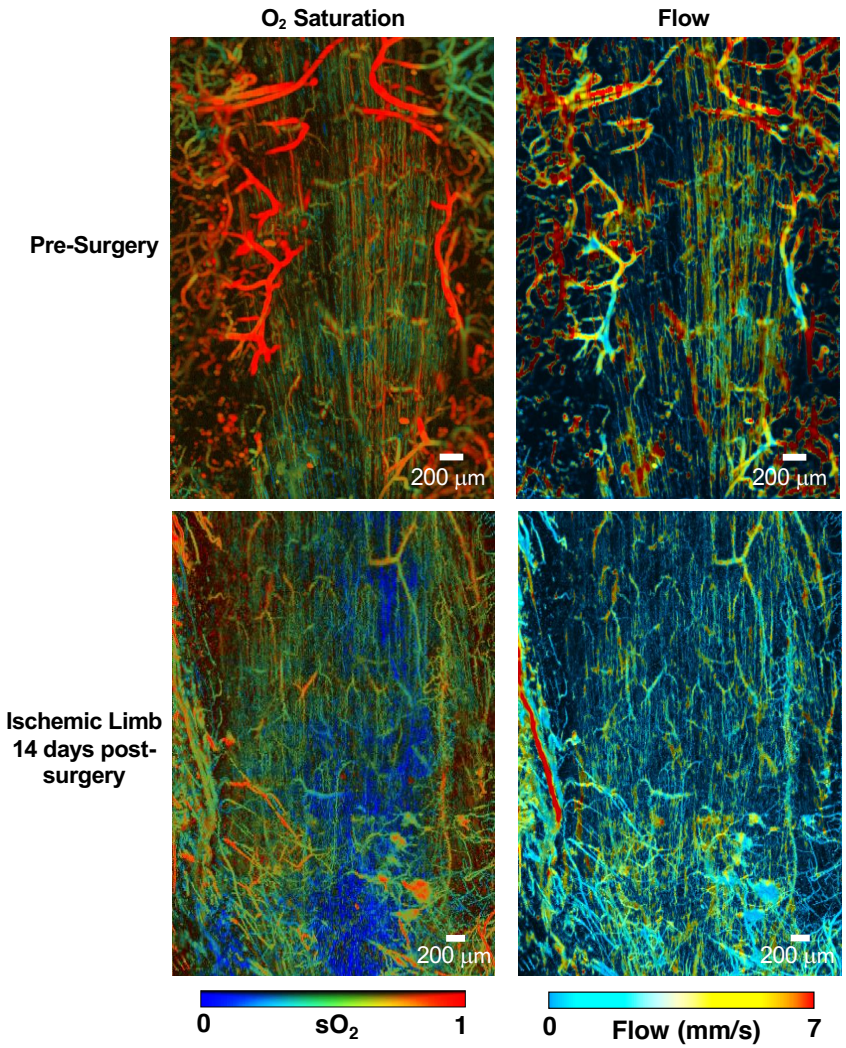

Figure 2-11 Photoacoustic Microscopy

Photoacoustic microscopy of the gastrocnemius before and 14 days after HLI. Oxygen saturation and flow remain reduced 14 days post-surgery and the vasculature is irregular and tortuous.

Discussion

In this study, we sought to evaluate perfusion measurement techniques in a mouse model of hindlimb ischemia. The three techniques utilized were LDPI, CEUS, and fluorescent microspheres. CEUS was shown to be well suited for hindlimb perfusion assessments. Variability in CEUS-derived perfusion ratios within and between mice, while greater than LDPI, is consistent with the variability in clinical perfusion values reported in human subjects.[61,62] In, mice CEUS enabled measurements of a cross-sectional view of both calves simultaneously, allowing for an internal control.

Since LDPI is the most common measurement method employed in HLI models, we next performed a direct comparison between CEUS and LDPI over a 150 day time course following the surgical induction of HLI. The LDPI perfusion recovery results are consistent with other reports from similar surgical procedures over the course of several decades.[14,16,29,64,65]

We were surprised to see a significant difference between LDPI and CEUS perfusion ratios at baseline, and that CEUS was consistently measuring a left to right ratio of about 1.2. To interrogate if this result was due to the imaging set up, we used a hydrophone to measure the peak negative pressure along the transducer. A left, center, and right measurement were taken and resulted in peak negative pressures of 0.2986, 0.3196, and 0.3084 MPa, respectively. These are relatively small differences and within an expected range of variation. We also changed the transducer orientation while imaging a mouse and quantified the results from each orientation. The transducer position had no effect on

the left:right perfusion ratio 1.102 vs 1.105 in the typical orientation vs opposite orientation. These results suggest that the transducer itself is not biasing the results, though they could be caused by another experimental factor. It is also possible that there is a real biological effect, or an environmental factor underlying this phenomenon.[66]

Even though the data does not suggest the baseline difference is due to the transducer, we decided to also analyze the data as a function of change from the pre-surgery perfusion ratios. To our surprise, both the non-normalized and normalized analysis showed that CEUS and LDPI have very different perfusion recovery kinetics and outcomes. The techniques differed at every time point (except day 4 post-surgery in the non-normalized analysis), although they did portray similar trends in recovery during the first week following surgery.

The most striking difference between the techniques is that by CEUS mice never fully recover perfusion in the ischemic hindlimb after surgery, and we validated this finding using a completely independent method (fluorescent microspheres). Histopathology and photoacoustic microscopy provide additional support by demonstrating abnormal muscle morphology and lower oxygenation and perfusion levels. This has significant implications for the field, and suggests that LDPI results (usually calculated from the feet) may not be representative of the physiology in the calves. This may partially explain some of the difficulties in translating preclinical successes to the clinic as the calves and thighs are the primary sites of atherosclerosis and vessel occlusion in PAD. A recent study by Arpino and colleagues using intravital microscopy to probe arterial morphology and function after

HLI in the extensor digitorum longus muscle is consistent with our findings, showing incomplete recovery up to 120 days post-surgery.[63] Their study, along with others, also document abnormal muscle morphology by histology at various time points that is consistent with our results showing irregular myofibers and centralized nuclei.[67,68]

To determine if the difference in perfusion recovery by CEUS and LDPI was due to the measurements being taken in different locations, perfusion recovery by LDPI was also measured in the calves. Perfusion recovery in the calves was very similar to that in the feet. The calves showed an even lower reduction in perfusion and faster recovery than the feet, which may be why most groups use the feet as an output because they allow for a greater dynamic range. This suggests that measurements by LDPI are independent of location below the level of the ligation. Other measurement factors associated with LDPI, such as the limited measurement depth, may contribute to the discrepancy compared to CEUS.

In the CEUS results, we observed an unexpected peak in the perfusion ratios on days 4 and 7 post-surgery. Based on previously studies employing LDPI, we had expected to see a nearly linear recovery in perfusion over time. A potential explanation for this is that, after the induction of ischemia, there is overgrowth and subsequent pruning of the vasculature coinciding with the increase and the decrease in perfusion. This was shown to occur by Landázuri and colleagues in a mouse model of hindlimb ischemia where the femoral artery and vein were ligated and excised.[69] Using micro-CT this group showed

that vascular volume, density, and connectivity peak at day 7 post-surgery and then decline.

Importantly, our findings suggest a more physiologically relevant model for testing therapeutic approaches to PAD. When using traditional LDPI, therapies are considered successful if they accelerate perfusion recovery since mice regain normal perfusion within a few weeks. This is not representative of what is happening in PAD patients, who experience a chronic and often declining disease state. Ironically, there is accumulating evidence to suggest that the mouse HLI model of PAD is actually quite faithful to the human disease process. When assessed by CEUS, this same mouse model appears to offer a more physiologically relevant test bed where mice reach a plateau in perfusion recovery that is more similar to reported patient outcomes.[70] We propose a new approach to evaluating therapies, where HLI surgery is performed, mice are allowed to reach a perfusion plateau, and then a therapeutic intervention is applied and assessed by CEUS. This method more accurately models the clinical condition and would allow for testing of therapies for their ability to improve perfusion rather than just accelerate perfusion recovery.

The use of CEUS to measure limb perfusion is not limited to animal research applications.[71,72] There are several groups that have used CEUS in humans to evaluate PAD.[26,27] Rather than the ratiometric assay used in preclinical studies where the unaffected limb serves as an internal control, clinical studies typically compare perfusion parameters before and after exercise stress.[73] These studies have shown a significant

differences between normal and PAD patients.[26,27] The successful use of CEUS in the clinical evaluation of PAD provides further confidence in the value of this technique in preclinical research.

To our knowledge this is the first study to provide a direct comparison of LDPI and CEUS, as well as the first study to show a persistent perfusion deficit by CEUS in a mouse model of hindlimb ischemia. We believe this may also be the first study to use repeated, label-free photoacoustic microscopy in a mouse model of HLI, although Ye and colleagues previously reported photoacoustic microscopy imaging at much lower resolution (and without oxygen saturation mapping) in a mouse model of HLI.[74]

In summary, this study aimed to evaluate perfusion measurement techniques used for mouse models of HLI. We showed that, despite being the most commonly used technique, the use of LDPI for perfusion measurements in a PAD model yields results that are inconsistent with CEUS, microsphere measurements, histopathology, photoacoustic microscopy, as well as clinical outcomes in PAD patients. These results provide a potential explanation for why the vast majority of therapies developed in the mouse HLI model ultimately fail in clinical trials, and suggest a new path forward for preclinical evaluation of therapeutics for the treatment of PAD.

Chapter 3 : Contrast Enhanced Ultrasound of Mouse Models of Hindlimb Ischemia Reveals Persistent Perfusion Deficit and Distinctive Muscle Perfusion Patterning

Introduction

Peripheral arterial disease (PAD) is caused by obstructive atherosclerosis leading to a lack of blood flow to the legs.[75] PAD can present with a variety of symptoms ranging from asymptomatic to intermittent claudication to the most severe form of the disease, critical limb ischemia, where gangrene may be present and necessitate amputation.[76] Very few therapies exist for PAD and using mouse models is an important component to increase understanding of the disease pathology to be able to bring new therapeutic approaches to the clinic.[75,77]

Mouse models of PAD are most often hindlimb ischemia (HLI) models where unilateral femoral artery ligation(s) and/or an excision of the femoral artery is performed.[17] Most commonly laser doppler perfusion imaging (LDPI) is used to measure perfusion recovery over time; however, we show in Chapter 2 that LDPI does not correlate with fluorescent microsphere, histological, or photoacoustic microscopy measurements of perfusion after HLI. We demonstrated contrast enhanced ultrasound (CEUS) did correlate well in an HLI model with a single femoral ligation. It is unknown what perfusion recovery responses would occur by CEUS with more severe HLI models that seek to represent more advanced forms of PAD.

Another advantage of using CEUS is that perfusion can be visualized in individual muscle groups. Spatial information about perfusion is lacking in the literature, as the techniques that can provide spatial information are typically destructive or limited to anatomical vascular structure rather than functional perfusion information. For example, Micro-CT and angiography can provide good anatomic structure, but limited functional perfusion information.[78] Other imaging techniques such as MRI or PET can provide spatial and perfusion information, but are much more costly and can suffer from poor resolution in small animals with low flow rates.[67] Compared to ultrasound, these techniques also require more resources and often dedicated personnel.

Here we evaluate perfusion recovery in two more severe mouse HLI models using CEUS. We compare the CEUS results with LDPI results. We also evaluate muscle perfusion patterns after surgery in three HLI models and use k-means clustering to identify groupings of mice that behave similarly after surgery.

Materials and Methods

Mice

Male C57BL/6 mice were purchased from Jackson Laboratory (Bar Harbor, ME, USA). Mice were provided with water *ad libitum* and standard chow. Mice were housed 1-4 animals per cage and in a room with a 12 hour light cycle. Standard corn cob bedding was used except post-surgery when iso pad bedding (Envigo, City, State, USA) was used until the mice were ambulating normally. The Institutional Animal Care and Use Committee of the University of Virginia approved all animal experiments.

Mouse Models of Hindlimb Ischemia

Mice (10-12 weeks old) were anesthetized with ketamine (90mg/kg) and xylazine (10 mg/kg). The left medial leg was shaved and depilated then the area was prepared for aseptic surgery. A heating lamp was used to maintain body temperature during surgery. An incision was made over the femoral artery and the following procedures for each type of surgery were followed (**Figure 3-1**):

Single ligation- 6-0 silk sutures were used to ligate the femoral artery proximal to the lateral circumflex femoral artery.[28]

Double ligation- 6-0 silk sutures were used to ligate the femoral artery proximal to the iliacofemoral artery and the popliteal/saphenous bifurcation.[28]

Excision- 6-0 silk sutures were used to ligate the femoral artery proximal to the pudendoepigastric trunk and the popliteal/saphenous bifurcation.[17,28]

Care was taken to not damage nearby structures such as the femoral nerve and vein. Bupenorphine-SR (0.5 mg/kg) was administered after surgery and readministered if needed. Mice were euthanized and excluded if necrosis reached the heel.

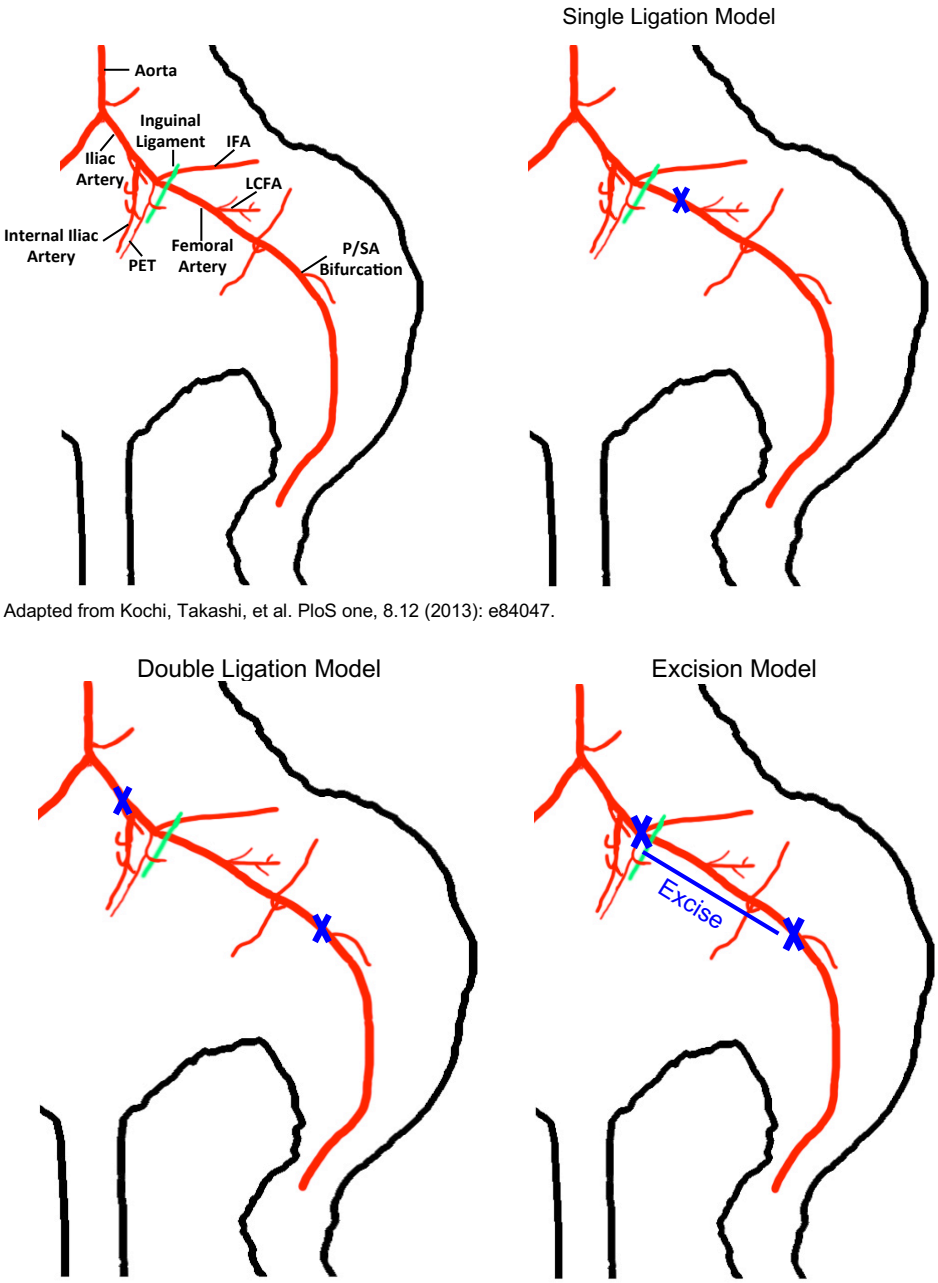

Figure 3-1 Three Ligation Models

The arterial anatomy of the mouse hindlimb. The single ligation, double ligation, and excision HLI models. An “X” denotes the location of a ligation and a line denotes the length of an excision.

Microbubble Preparation

Microbubbles were prepared as previously described by using decafluorobutane gas, which was dispersed in saline by sonication.[55] Microbubbles were stabilized with a lipid monolayer that contained 1,2-distearoyl-*sn*-glycero-3-phosphocholine (DSPC) and PEG stearate. To ensure microbubbles do not get trapped in the lungs, the presence of any larger than 7 μm was minimized by flotation at normal gravity. The vial concentration was measured approximately every two weeks (Beckman Coulter, Indianapolis, Indiana, USA). Microbubbles were diluted with sterile saline directly before administration, if required.

Contrast Enhanced Ultrasound

Imaging was performed on an Acuson Sequoia C512 system with a 15L8W transducer (Siemens, Munich, Germany) as previously described in Chapter 2. Briefly, mice were anesthetized with 1-2% isoflurane in air, placed prone on a heated stage with legs extended, and the feet were secured. A catheter with a 27G catheter filled with heparinized saline (100 units/ml) was inserted in the tail vein and secured. The transducer was positioned across the calves and previously optimized scanning parameters were used (frequency: 7 MHz, dynamic range: 100 dB, gain: -10, imaging mechanical index: 0.2, burst mechanical index: 1.9, and burst time: one second). Video of the ultrasound imaging was captured in real time. The microbubble solution ($1x10^7$ MB/min) was infused via tail vein catheter. After reaching steady state, burst pulses were applied once per minute for 10-15 minutes, these pulses cause the microbubbles in the field of view to

burst. Microbubbles from upstream continue to flow into the scanning plane, and enable perfusion to be quantified.[22]

A custom MATLAB (Mathworks, Natick, Massachusetts, USA) script was used for analysis as previously described in Chapter 2. The image intensity over time of each flash-replenishment sequence was fit to $y=A(1-e^{-\beta t})$ where A represents blood volume, beta represents blood velocity, and $A*\beta$ represents blood flow.[22] The average ischemic:control $A*\beta$ ratio was used as the CEUS output metric.

Perfusion Pattern Analysis

CEUS imaging data day 1 post-surgery was used for pattern analysis. 46 mice (17 single ligation, 18 double ligation, and 11 excision) were analyzed. A B-mode image, a contrast mode image before microbubble infusion (background), and a contrast mode image during steady state microbubble infusion were extracted from the video data for each mouse. Data were analyzed using a custom MATLAB (Mathworks, Natick, Massachusetts, USA) script. The background image was subtracted from the contrast image to ensure any artifacts were removed before quantification. The B-mode image was used to determine the region of interest in the same way as was done with the video data. The region of interest was further broken into four major muscle groups plus the skin based on published microscopy images of the mouse hindlimb.[79] Smaller muscles were excluded because they are difficult to correctly segment and contribute minimally to the total signal. The average image intensity in each muscle region was then quantified.

k-means clustering was performed on these muscle region intensities for two to ten clusters. The number of clusters was optimized by maximizing the mean silhouette score.

Histological Analysis

Mice were anesthetized with ketamine (90mg/kg) and xylazine (10 mg/kg). Mice were perfused through the left ventricle with heparinized saline (10 units/ml) and then 4% paraformaldehyde. Skeletal muscles of the calf were harvested and incubated in 4% paraformaldehyde at 4℃ for 48-72 hours. The tissue was then rinsed three times in saline and then placed in 15% sucrose overnight followed by 30% sucrose overnight. Tissue was flash frozen in OCT, 10 μm sections were cut and stained with H&E.

Statistical Analysis

All results are presented as mean±SEM. A linear mixed model with Bonferroni correction was used to analyze the longitudinal LDPI and CEUS data using SAS version 9.4 (SAS Institute, Inc., Cary, NC, USA). Comparisons between more than two groups were performed with a one-way ANOVA and post-hoc analysis (Tukey's test) as appropriate. $P<0.05$ was considered significant. Except as noted, GraphPad Prism version 5.0 (GraphPad Software, San Diego, CA, USA) was used to perform statistical analyses.

Results

The imaging set up and muscle regions are shown in **Figure 3-2**. Based on microscopy images of the mouse calf, the locations of different muscle groups on the ultrasound images could be determined (**Figure 3-3**).[79] Several small muscles were difficult to place individually and were grouped with other muscles or not included because they did not significantly contribute to the ultrasound signal.

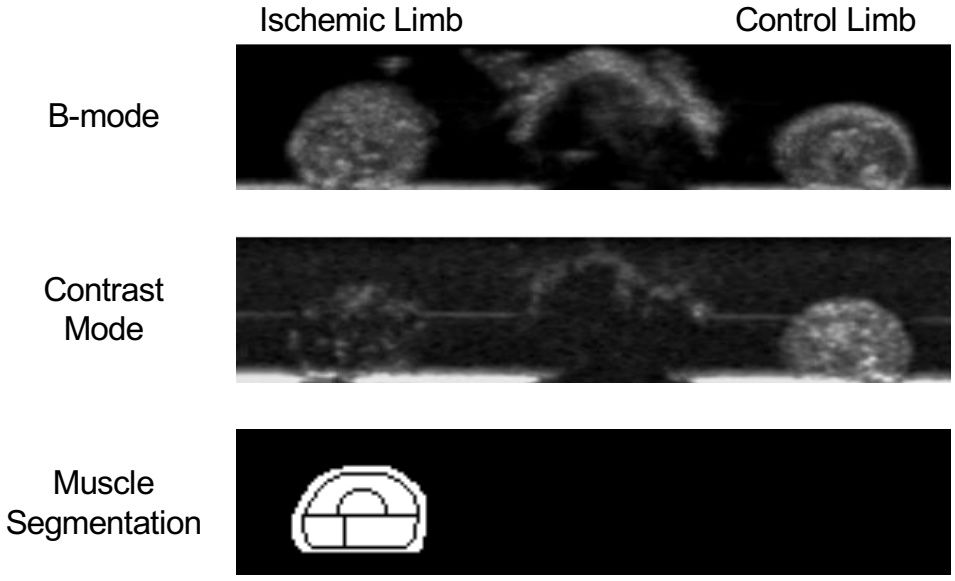

Figure 3-2 Ultrasound Imaging Setup

Example images of a mouse one day after excision surgery. The B-mode image was used to define the muscle segmentation. The contrast mode shows that there is almost no flow in the ischemic limb.

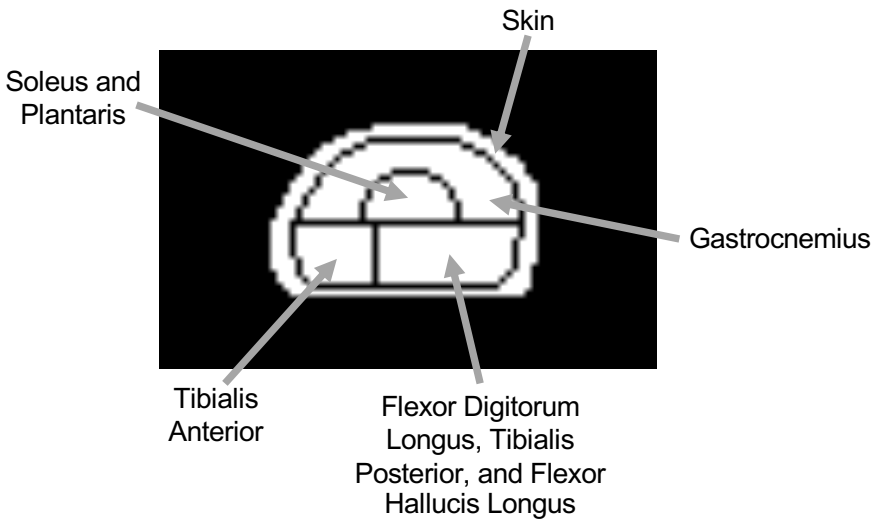

Figure 3-3 Muscle Segmentation

Schematic of the muscle groupings in the left mouse hindlimb used for clustering analysis. Only the major muscle groups are shown.

Double Ligation Surgery Results in Sustained Perfusion Deficit

To evaluate perfusion recovery over time in the double ligation HLI model, mice were imaged at baseline and days 1, 4, 7, 14, 28, 60, 90, and 150 after surgery by LDPI and CEUS (**Figure 3-4**). By LDPI, perfusion in the ischemic limb was reduced to 35% of the control limb day 1 post-surgery. Perfusion in the ischemic limb then increased approximately linearly until day 14 post-surgery, at which time it returned to pre-surgery levels and remained steady through day 150 post-surgery. By CEUS, perfusion in the ischemic limb was reduced to 6% of the control limb on day 1 post-surgery. In contrast to LDPI, by CEUS perfusion in the ischemic limb modestly peaked at 52% days 7 and 14 post-surgery and then plateaued at ~35% of the control limb through the end of the study.

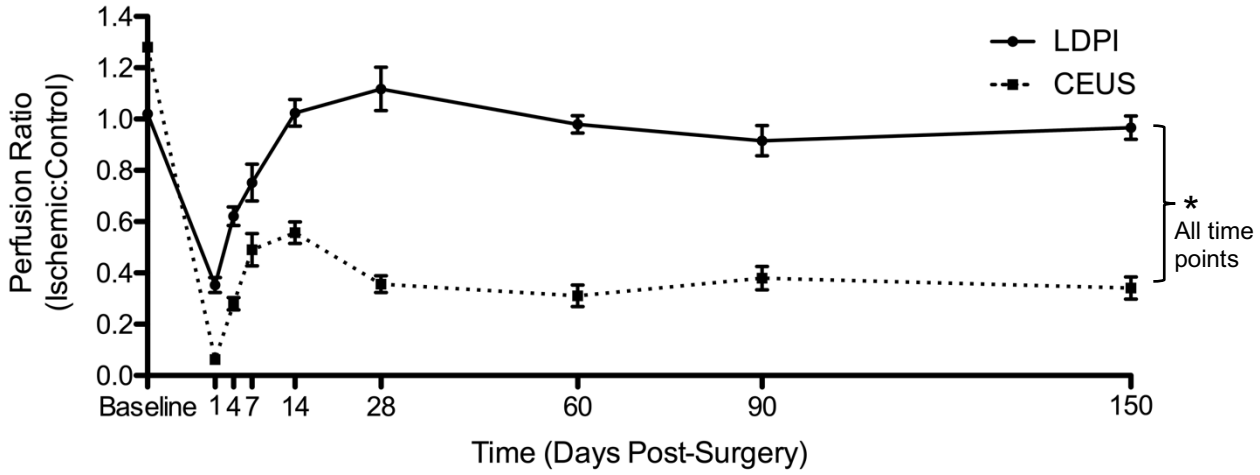

Figure 3-4 Perfusion Recovery After Double Ligation HLI

The ratio of perfusion in the ischemic:control limb measured by LDPI and CEUS at baseline and days 1, 4, 7, 14, 28, 60, 90, and 150 after double ligation surgery. By LDPI perfusion returns to normal within 14 days post-surgery. However, by CEUS perfusion in the ischemic limb modestly peaks at days 7 and 14 and then plateaus at ~35% of the control limb through the end of the study. Measurements by LDPI and CEUS are significantly different at all time points (*$p<0.01$; n=16-18 for baseline to 14 day time points, n=8 for 28-150 day time points). Statistical analysis was performed using a linear mixed model with Bonferroni correction.

Excision Surgery Results in Sustained Perfusion Deficit

To evaluate perfusion recovery over time in the excision HLI model, mice were imaged days 1, 4, 7, 14, and 28 after surgery by LDPI and CEUS (**Figure 3-5**). Baseline data was not acquired for this group of mice, however we use the previously acquired average baseline data from 35 mice as a reference group. By LDPI, perfusion in the ischemic limb was reduced to 36% of the control limb day 1 post-surgery. Perfusion in the ischemic limb then increased approximately linearly until day 14 post-surgery, at which time it returned to pre-surgery levels and remained steady until day 150 post-surgery. By CEUS, perfusion in the ischemic limb was reduced to 5% of the control limb on day 1 post-surgery. In contrast to LDPI, by CEUS perfusion in the ischemic limb modestly peaked at 54% day 7 post-surgery and then plateaued at ~41% of the control limb through the end of the study.

Pathological Muscle Morphology

H&E staining was used to evaluate muscle morphology in control and ischemic limbs at day 150 post-surgery for the double ligation surgery and at day 28 post-surgery for the excision surgery (**Figure 3-6**). Ischemic limb muscle from both surgeries shows irregular fiber structure and fibers with centralized nuclei. In control limbs from both surgeries, there is more consistent fiber organization and most muscle fibers have peripheral nuclei.

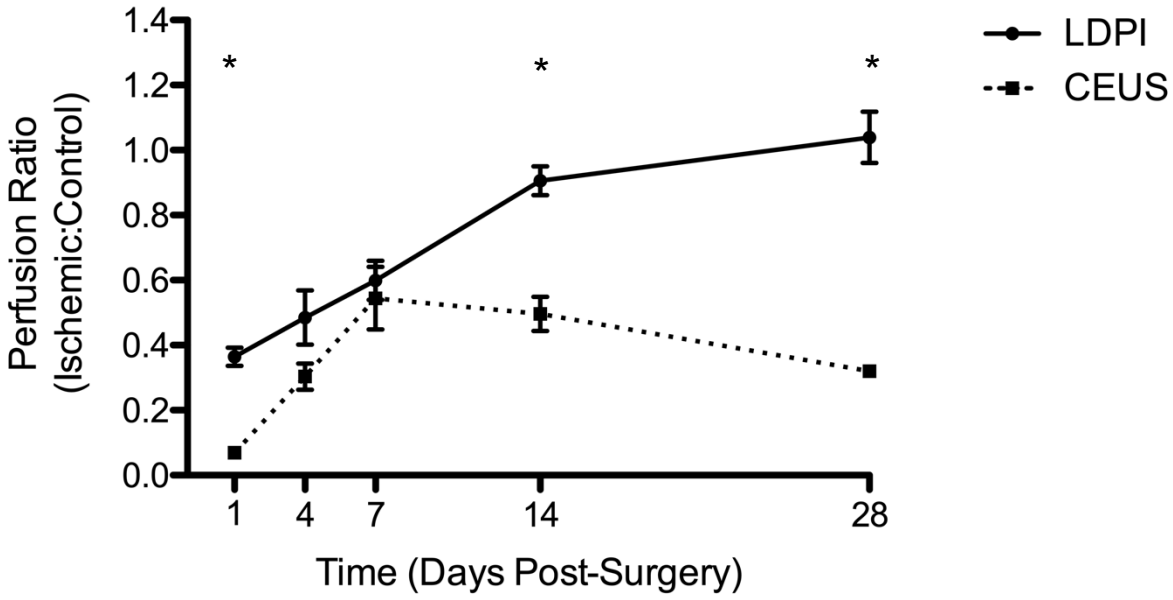

Figure 3-5 Perfusion Recovery After Excision HLI

The ratio of perfusion in the ischemic:control limb measured by LDPI and CEUS at baseline (from reference group) and days 1, 4, 7, 14, and 28 after excision surgery. By LDPI perfusion returns to normal within 14 days post-surgery. However, by CEUS perfusion increases until day 7 post-surgery. Day 14 and 28 post-surgery slightly decrease and average 41% of the control limb. (*$p<0.01$, $n=11$. Statistical analysis was performed using a linear mixed model with Bonferroni correction.

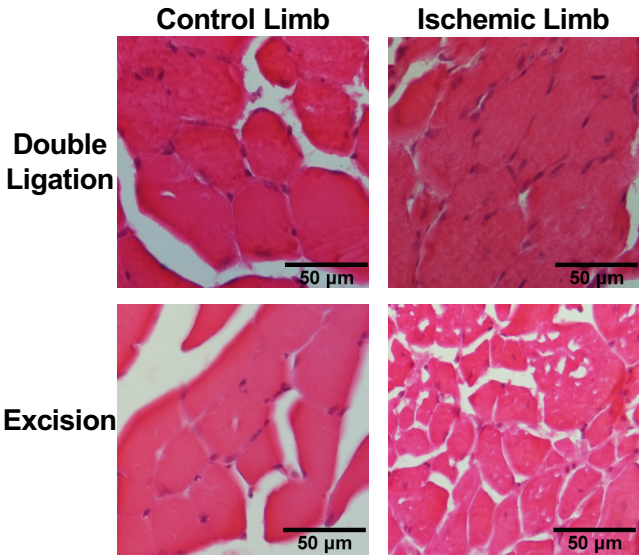

Figure 3-6 Muscle Morphology After Double Ligation and Excision Surgeries

H&E staining of muscle 150 days after double ligation surgery and 28 days after excision surgery at 200x. Representative control limb muscle shows peripheral nuclei and uniform myofiber architecture. Representative ischemic limb muscle from both surgeries shows irregular myofibers and many myofibers with centralized nuclei.

Perfusion Patterns are Conserved Across HLI Models

It was clear during CEUS imaging day 1 post-surgery that not every mouse responded the same way to a given surgery. While all mice had a very significant decrease in perfusion, different mice had different regions of the limb that were more or less perfused compared to others. It also seemed like there may be some conserved patterns of perfusion. To quantitatively assess these patterns k-means clustering was used (**Figure 3-7**). The optimal number of clusters was determined to be five. The single ligation surgery contained all five of the clusters (1, 2, 3, 4, 5). The double ligation surgery contained three of the clusters (2, 3, 5). The excision surgery contained three of the clusters (3, 4, 5). Cluster 1 corresponds to no perfusion in the tibilais anterior. Cluster 2 corresponds to perfusion to all muscles. Cluster 3 corresponds to perfusion only to the gastrocnemius. Cluster 4 corresponds to no perfusion to the tibilias anterior, flexor digitorum longus, tibialis posterior, and flexor hallucis longus. Cluster 5 corresponds to little to no perfusion in any muscle with minimal perfusion to the skin.

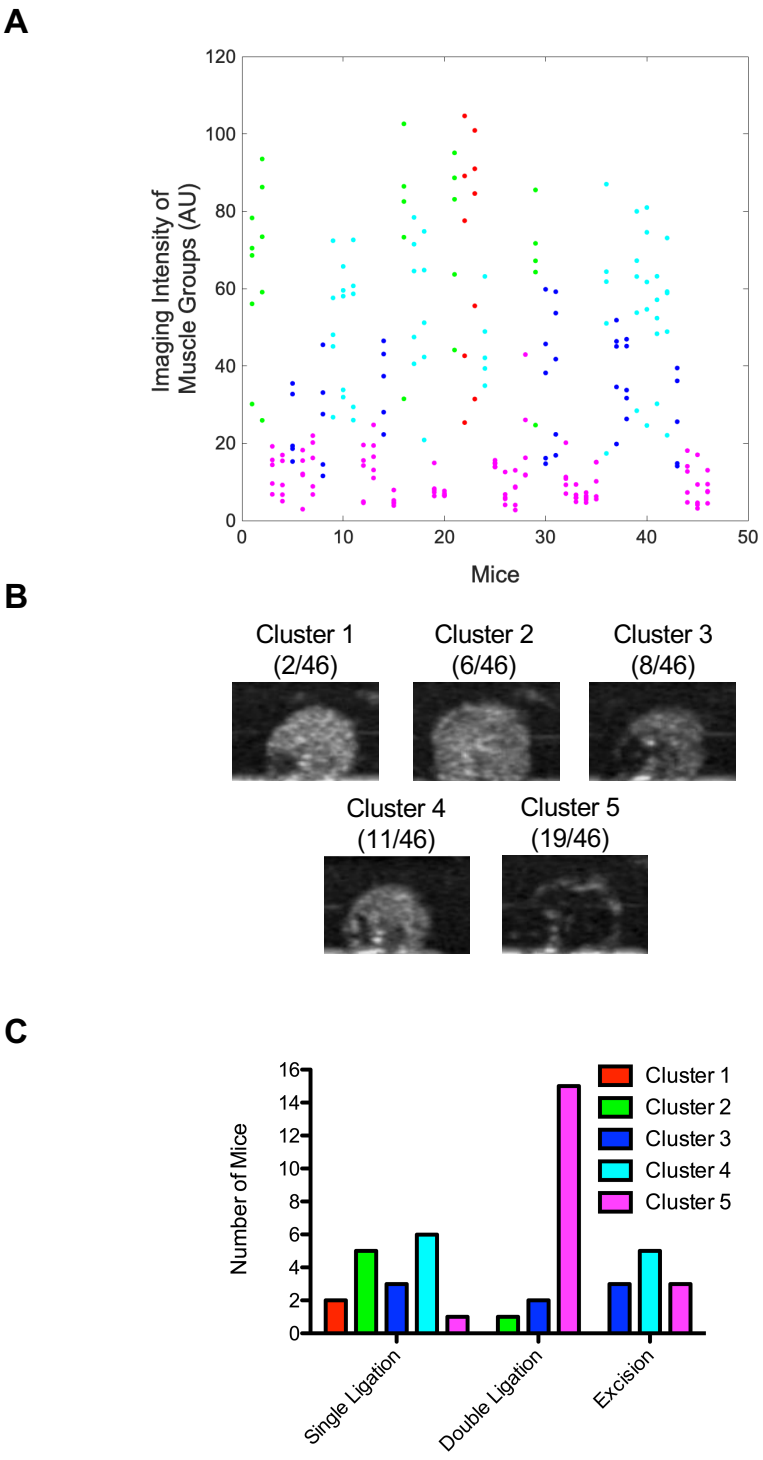

Figure 3-7 Perfusion Cluster Analysis

A) Visualization of the clustered data. Each data point is the mean signal intensity of a muscle group and each color is a different cluster. B) A representative contrast mode image and number of mice in each cluster identified. C) The distribution of clusters within each type of surgery.

Discussion

In this study we sought to evaluate two mouse models of hindlimb ischemia, continuing our work in exploring the use of CEUS to study PAD. In Chapter 2 we validated CEUS in a single ligation HLI model with fluorescent microspheres, histopathology, and photoacoustic microscopy, and showed that LDPI results were inconsistent with these validation techniques. Here we measured perfusion recovery in two more severe models of HLI with LDPI and CEUS.

Assessment using LDPI shows perfusion increases in the ischemic limb until day 14 post-surgery where it returns to pre-surgery levels in both the double ligation and excision models. In contrast, by CEUS perfusion in the ischemic limb increases until day 14 post-surgery and it then levels off to about 40% of the control limb, never returning to normal in both the double ligation and excision models. By CEUS we observe a peak in perfusion in the ischemic limb at days 7 and 14 of 52% after double ligation surgery and a peak 7 days post-surgery of 54% after excision surgery. These results are all consistent with the pattern of recovery measured by LDPI and CEUS in Chapter 2 using a single ligation model of HLI. With the addition of the double ligation model and the excision model we have covered the range of severity that is typical of studies using an HLI model. This further extends the impact of our findings as being broadly applicable in HLI models employing unilateral femoral artery ligation and excision techniques.

One of the advantages of using CEUS is that when the transducer is positioned across the calves the differential perfusion to individual muscle groups can be seen. This is

especially prominent when imaging 1 day post-surgery. k-means clustering of all the day 1 post-surgery images for the three surgeries reveals 5 predominant patterns, most of which occur in multiple surgery conditions. This was an unexpected finding that the same surgery could produce vastly different results in different mice. We hypothesize that this variation is due to innate differences in where arteries branch off as well as collateralization that allows some mice to retain different levels of muscle perfusion after surgery.[28] Other groups have shown that different mouse strains recover from HLI differently based on innate collateralization, it is possible a similar affect occurs on a per-mouse basis within the same strain to a lesser extent.[29,80,81] We did not observe any patterns in the recovery time course based on the initial muscle perfused. However, it is possible that the microenvironment of these patterns is different and may have implications for the response to different therapies under investigation. This also has implications for assays that require the sampling of muscles, where results might vary as a result of the initial state of perfusion after HLI.

To our knowledge this is the first study to use CEUS to evaluate different HLI surgeries. We believe that this is also the first study to demonstrate different muscle perfusion patterns in mouse models of hindlimb ischemia.

This study aimed to evaluate two severe models of hindlimb ischemia with CEUS. We show that, contrary to LDPI results, perfusion never fully recovers after surgery. We also show that individual mice can have drastically different muscle perfusion pattern responses to the same surgery. These results have significant implications for the

evaluation of therapeutics to treat PAD, and more research needs to be done to elucidate the effects of variable responses to surgery.

Chapter 4 : Evaluating Antioxidant Therapies in a Mouse Model of PAD

Introduction

The prevalence of peripheral arterial disease (PAD) is >10% of people over 60 years old, and increases with age.[8] PAD patients can experience significant reductions in quality of life, yet there are relatively few treatments available.[82,83] The current best medial management includes the reduction of risk factors such as quitting smoking, managing diabetes, reducing blood pressure, and reducing cholesterol.[77] Exercise, particularly supervised exercise, has long been recognized as an effective method to reduce symptoms.[84–86] However, patient compliance can be low and not all patients are able to perform exercise.[87] There is only one medication, cilostazol, shown to be effective in modestly increasing pain free walking distance.[10,88] There are also several surgical and endovascular procedures used to treat PAD.[89] Revascularization can involve endarterectomy, bypass, stenting, and/or angioplasty.[12,89] Surgical interventions can be very successful, but many patients are not candidates and there can be significant surgical complications.[90,91]

More effective therapies are needed to treat all stages of PAD. There have been dozens of clinical trials investigating promising strategies for therapeutic angiogenesis.[15,75,92] These clinical trials primarily evaluate protein therapy, cell therapy, gene therapy or a combination of these therapies.[92] The most common proteins and associated genes are growth factors such as: vascular endothelial growth factor (VEGF), fibroblast growth

factor (FGF) and hepatocyte growth factor (HGF).[92,93] Unfortunately, trials targeting these growth factors, and many others, have not proven to be efficacious in humans.[15,92,93]

When evaluating potential therapies, mouse models of hindlimb ischemia are often used. Typically, the primary output of these studies is the acceleration of perfusion recovery assessed by LDPI. As we have shown previously, LDPI is not representative of other established metrics to assess perfusion recovery. This may contribute to the failure of many clinical trials for PAD. There are a variety of emerging therapeutic strategies such as miRNA, antioxidants, and stem cell therapies that would benefit from evaluation with CEUS.[94–96] Here we will evaluate the efficacy of two antioxidant therapies, N-(2-mercaptoptopionyl)-glycine (MPG) and alpha lipoic acid (LA), with CEUS in a single ligation mouse model of HLI.

Materials and Methods

Mice

C57BL/6 male mice were purchased from Jackson Laboratory (Bar Harbor, ME, USA). Mice were provided standard chow and water ad libitum. They were housed 1-4 per cage in a room with a 12 hour light cycle. Cages contained corn cob bedding except during surgical recovery where iso pad bedding (Envigo, City, State, USA) was used until mice were ambulating normally.

Mouse Models of Hindlimb Ischemia

10-12 week old mice were anesthetized with ketamine (90mg/kg) and xylazine (10 mg/kg). The single ligation surgery was performed as previously described in Chapter 2.

Laser Doppler Perfusion Imaging (LDPI)

Mice were anesthetized with 1-2% isoflurane and imaged with the LDPI instrument (Perimed, Sweden), as previously described in Chapter 2. Three to five measurements were taken, about one minute apart. Data were analyzed using the included PimSoft analysis software. ROIs were selected around the feet, the image intensity was averaged over all measurements, and a ratio of left:right (ischemic:control) foot was calculated.

Microbubble (MB) Preparation

Microbubbles were prepared from decafluorobutane gas, which was dispersed in normal saline by sonication, as previously described in Chapter 2.[55] The vial concentration was measured approximately every two weeks using a Coulter Counter (Beckman Coulter, Indianapolis, Indiana, USA). If needed, the microbubbles were diluted with sterile saline just before use.

Contrast Enhanced Ultrasound (CEUS)

Imaging was performed with an Acuson Sequoia C512 system and a 15L8W transducer (Siemens, Munich, Germany) as previously described in Chapter 2.

Video data were analyzed using a custom MATLAB (Mathworks, Natick, Massachusetts, USA) script as previously described in Chapter 2. Briefly, image intensity over time was calculated and each flash-replenishment sequence was separated to allow for curve fitting. The data were fit to $y=A(1-e^{-\beta t})$ where A represents blood volume, β represents blood velocity, and $A*\beta$ represents flow.[22] The average left:right (ischemic:control) $A*\beta$ ratio was calculated for direct comparison with LDPI.

Administration of MPG and LA

Mice were injected subcutaneously with saline, MPG (20 mg/kg, Millipore Sigma, Burlington, MA, USA), or LA (0.1 mg/kg, Millipore Sigma, Burlington, MA, USA) daily from day 14 to day 27 post-surgery.[97,98] Injections were performed at approximately the same time each day.

Histological Analysis

Tissue harvesting and preparation for sectioning was performed as previously described in Chapter 2. 10 μm sections were cut and stained with H&E.

Results

MPG Administration Does Not Affect Perfusion Recovery

Day 1 and 14 post-surgery time points are consistent with previous results from the single ligation surgery (**Figure 4-1**). Day one post-surgery there is a significant decrease in perfusion which increases to ~56% on day 14 post-surgery. The administration of MPG shows no improvement in perfusion over saline administration. The perfusion ratio of the

ischemic limb on days 7 and 14 of MPG administration (days 21 and 28 post-surgery) is 43% of the control limb.

Lipoic Acid Administration Does Not Affect Perfusion Recovery

Day 1 and 14 post-surgery time points are consistent with previous results from the single ligation surgery (**Figure 4-2**). Day 1 post-surgery there is a significant decrease in perfusion which increases to 51% on day 14 post-surgery. The administration of LA shows no improvement over saline administration. The perfusion ratio of the ischemic limb to the control limb on days 7 and 14 of LA administration (days 21 and 28 post-surgery) is 55% and 53%, respectively.

A closer look at the data reveals one mouse that shows a pattern of perfusion recovery that could be consistent with the drug having an effect (**Figure 4-3**). In contrast to the typical perfusion ratio of 50-60%, this mouse had a ratio of 33% perfusion compared to the control limb. After drug administration, perfusion rose to 63% and 62% of the control on days 21 and 28 post-surgery, respectively.

Pathological Muscle Morphology

Muscle morphology in control and ischemic limbs from all treatment conditions was evaluated with H&E staining day 28 post-surgery (**Figure 4-4**). Consistent with our previous histological findings, muscle from the ischemic limbs showed irregular fibers and many fibers with centralized nuclei. In control limbs, the majority of muscle fibers have peripheral nuclei and have a more consistent fiber arrangement.

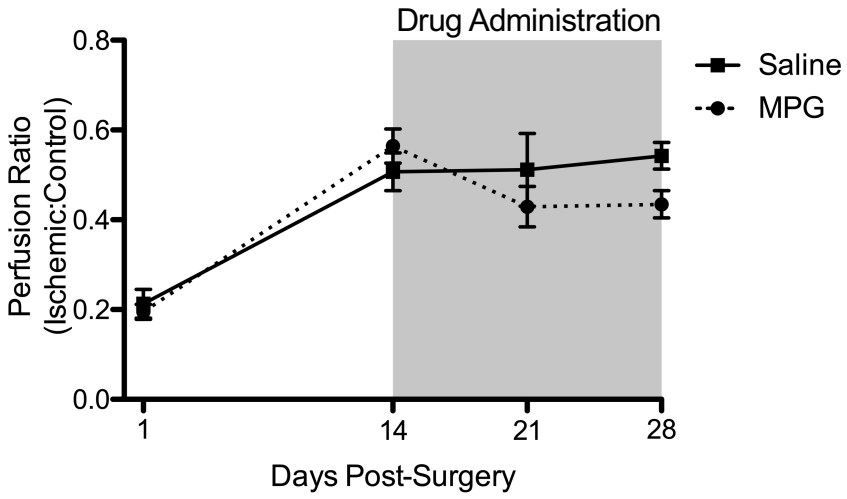

Figure 4-1 MPG Administration Does Not Affect Perfusion Recovery

The ratio of perfusion in the ischemic:control limb measured by CEUS at days 1, 14, 21, and 28 after single ligation surgery with daily saline or MPG administration from 14-28 days. The administration of MPG shows no improvement in perfusion over saline administration. (MPG n=6, Saline n=5)

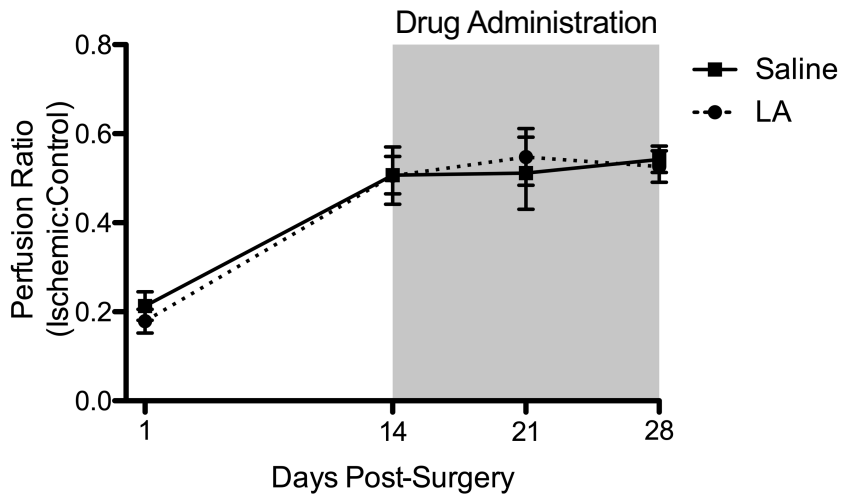

Figure 4-2 LA Administration Does Not Affect Perfusion Recovery

The ratio of perfusion in the ischemic:control limb measured by CEUS at days 1, 14, 21, and 28 after single ligation surgery with daily saline or LA administration from 14-28 days. The administration of LA shows no improvement in perfusion over saline administration. (LA n=6, Saline n=5)

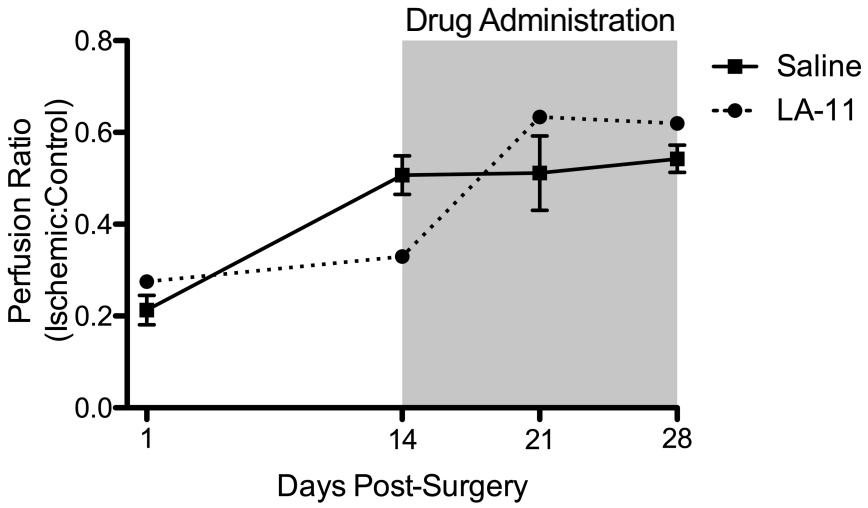

Figure 4-3 Individual Response to LA Administration

The ratio of perfusion in the ischemic:control limb measured by CEUS at days 1, 14, 21, and 28 after single ligation surgery with daily saline or LA administration from 14-28 days. The LA data is from a single mouse that shows increases perfusion in the ischemic limb after LA administration. (Saline n=5)

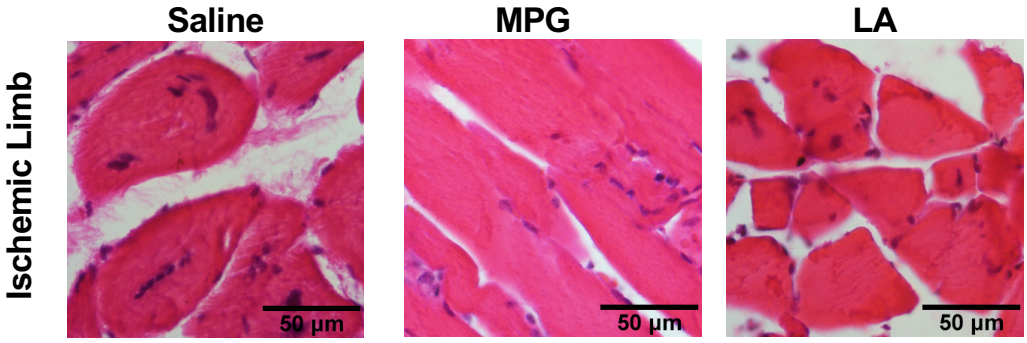

Figure 4-4 Muscle Morphology After Drug Treatment

H&E staining of muscle 28 days after single ligation surgery at 200x. Representative ischemic limb muscle from the saline, MPG, and LA groups are similar and show irregular myofibers and many myofibers with centralized nuclei, indicating that neither MPG nor LA improved muscle morphology.

Discussion

In this study we sought to use CEUS to evaluate antioxidant therapies in a mouse HLI model. MPG, LA, and a saline vehicle control were injected daily from 14-28 days post-surgery. The saline control injection resulted in a similar mean perfusion recovery as we have previously shown in untreated mice.

There have been three surgeries presented in detail in this dissertation. While the exact percentage of the perfusion plateau reached varied slightly, in all three surgeries perfusion in the ischemic limb was significantly lower. It is unknown if the microenvironment from one of these surgeries is more similar to PAD, thus we chose the single ligation model for practical reasons. The single ligation model is a technically less difficult procedure to perform with a lower risk of complications such a bleeding. This model also does not result in the severe necrosis that can occur with the double ligation and excision models, necessitating euthanasia.

Evidence suggesting an effective therapy would be an increase in perfusion in the ischemic:control perfusion ratio at the day 21 and 28 post-surgery imaging time points. The MPG treated mice showed no change in perfusion at either time point. There was also no improvement noted in the histological sections. Similarly, the LA treated mice showed no improvement in perfusion or muscle morphology in histological sections.

When looking at data from individual mice, one LA treated mouse did seem to have an increase in the ischemic:control perfusion ratio at the day 21 and 28 post-surgery time

points, indicating a possible effect of the drug treatment. This mouse was unique in that at day 14 post-surgery it had a low perfusion ratio compared to the saline control (0.33 vs 0.51±0.04). It is possible that the lower perfusion at day 14 provided an environment for the LA therapy to be modestly effective. However, the limited number of animals in this study makes it difficult to evaluate whether this mouse is an outlier. Applying the same treatment strategy in a more severe HLI model would help discern the effect of LA administration. In addition, future studies could include a range of dosages, treatment lengths, and routes of administration.

Despite the largely negative results of these antioxidants, using CEUS to evaluate other therapies in this manner is a valuable tool. Improving perfusion, rather than accelerating perfusion recovery, presents a more realistic model of the therapeutic need that PAD patients have. This may reduce the amount of time and money wasted on failed clinical trials.[99]

Chapter 5 : Conclusions and Future Directions

In this dissertation we sought to develop and evaluate CEUS for the assessment of perfusion recovery in mouse hindlimb ischemia models of PAD. Mouse models are a valuable tool to study underlying disease mechanisms and evaluate potential therapies. The use of CEUS in HLI models was hypothesized to provide additional information that other techniques, particularly LDPI, could not measure. Surprisingly, we found that CEUS revealed a contrary picture of the pathophysiology in HLI models, and provided a way to critically evaluate the current state of PAD research.

Our first unexpected finding was that CEUS and LDPI show different time courses of perfusion recovery after HLI. Our LDPI measurements, in agreement with the literature, showed that perfusion fully recovered one to two weeks post-surgery.[29,100] In contrast, CEUS showed incomplete recovery (~50%) by two weeks post-surgery. The CEUS findings were validated by fluorescent microsphere measurements, histology, and photoacoustic microscopy.

Another related finding is that by CEUS the ischemic limb never fully recovers, remaining at 35-55% of normal 5 months post-surgery, depending on the surgery performed. This again differs from our LDPI results and the literature. Another independent method, intravital microscopy, recently demonstrated the presence of a flawed microcirculation in agreement with our results.[63] These findings provide an opportunity to reconsider the reliance on LDPI measurements as the primary endpoint in HLI studies.

When using LDPI, therapies are considered successful if they accelerate perfusion recovery, as mice regain normal perfusion within a few weeks after surgery. This is not representative of the pathophysiology in PAD patients, who experience a chronic and often declining disease state. When assessed by CEUS, HLI models appear to offer a more physiologically relevant test bed where mice reach a plateau in perfusion recovery that is more similar to patient outcomes.[70] We propose a new approach to evaluate therapies, where HLI surgery is performed, mice are allowed to reach a perfusion plateau, and then a therapeutic intervention is applied and assessed by CEUS. This method more accurately models the clinical condition and would allow for testing of therapies for their ability to improve perfusion rather than just accelerate perfusion recovery.

We also show that muscle-specific perfusion patterns occur on day one after HLI, and that most of these patterns are conserved across multiple surgeries. We believe this is the first report that HLI surgery can cause differences in individual muscle perfusion in different mice. This has implications for assays that require the sampling of muscles, where results might vary as a function of the initial state of perfusion after HLI. This phenomenon is potentially due to differences in the location that certain major arteries arise, which varies between mice and occurs in the regions where ligations are made.[28] It could also be due to differences in innate collateralization in the arterioles and capillaries, similar to what is seen when comparing different strains of mice.[29,80] Since this analysis was performed retrospectively we can only speculate on the mechanism. In the future, analysis of the arterial anatomy could be performed during surgery and then compared to the resulting perfusion patterns to look for potential relationships.

A number of additional questions have arisen from these studies that merit further investigation. One intriguing finding is that the baseline CEUS data consistently shows a ~20% perfusion bias towards the left limb. Hydrophone and in vivo measurements in both orientations suggest that it not a function of the transducer, but other unknown experimental, biological, or environmental factors may contribute. Further experimentation to evaluate these unknown factors is warranted.

We also report a modest peak in perfusion by CEUS at about 1 week post-surgery for all three HLI models. This is consistent with micro-CT results that show vascular, volume, density, and connectivity peak at one week post-surgery, followed by pruning.[69] A more full picture of the microenvironment of the ischemic limb would provide insight into why this peak occurs, as well as how successfully HLI models represent human PAD. A particularly interesting avenue to investigate is the immune response after HLI. There have been several studies using various knockout mouse models that demonstrate perfusion recovery can be modulated by the immune system.[64,101–103] It is also well known ischemic vascular diseases, including PAD, have significant immunologic components to pathology.[104]

Future work should also be focused on using HLI mouse models in conjunction with CEUS to evaluate novel therapeutic approaches for the treatment of PAD. There are many options to consider, and given the difficulty thus far in developing effective therapies it is likely that new approaches are needed. miRNA and oxidative stress are both attractive targets for future therapies.[94,95] There is also the potential for novel gene therapies and

cell therapies to prove effective.[105] Different vehicles such as nanoparticles may be useful in increasing drug delivery.[106] All of these options are suited to evaluation by CEUS mouse models of HLI.

In summary, this dissertation provides a novel evaluation of preclinical PAD models using CEUS. We demonstrate not only that CEUS is well suited for measurements of perfusion in HLI models, but also that it yields a more relevant assessment with respect to the clinical condition. These studies provide a novel framework for assessing perfusion recovery in HLI models; enabling the field to continue moving forward to develop greatly needed therapies.

Appendix A: Derivation of CEUS Fitting Equation From a Single Compartment Model

We assume that the imaging plane can be reasonably modeled as a single inlet with concentration (C_{A1}) and single outlet. We also assume a well mixed system with constant volume (V), constant flow (Q_v), constant rate of infusion, no reacting species, and an impermeable wall. Equation 2 describes the concentration (C_A) of a species A, over time in this single compartment model with the above assumptions.[107]

$$V\frac{dC_A}{dt} = Q_V(C_{A1} - C_A) \tag{2}$$

Since the inlet concentration (C_{A1}) does not change over time Equation 2 can be rewritten as Equation 3.[107]

$$\frac{d(C_A - C_{A1})}{C_A - C_{A1}} = -\frac{Q_V}{V}dt \tag{3}$$

Knowing an initial concentration (C_{A0}) we can integrate to get[107]:

$$\frac{C_A - C_{A1}}{C_{A0} - C_{A1}} = e^{-\frac{Q_V}{V}t} \tag{4}$$

Since curve fitting is done starting after each high power burst pulse we know C_{A0}=0, simplifying to Equation 5.

$$\frac{C_A - C_{A1}}{-C_{A1}} = e^{-\frac{Q_V}{V}t} \tag{5}$$

This equation can be written into the form of the exponential fit equation used for CEUS (Equation 6).

$$C_A = C_{A1}(1 - e^{-\frac{Q_V}{V}t}) \tag{6}$$

Q_V/V is flow over volume and reduces to units of 1/time, analogous to beta in the fitting CEUS fitting equation.[22] The concentrations in this equation are represented as image intensities in the ultrasound data. C_{A1} is analogous to the A coefficient which is the plateau of image intensity and a representation of blood volume since the system is assumed to be well mixed.[22]

References

1. Fowkes FGR, Rudan D, Rudan I, Aboyans V, Denenberg JO, McDermott MM, Norman PE, Sampson UK, Williams LJ, Mensah GA, Criqui MH. Comparison of global estimates of prevalence and risk factors for peripheral artery disease in 2000 and 2010: a systematic review and analysis. *The Lancet*. 2013;382(9901):1329-1340. doi:10.1016/S0140-6736(13)61249-0.

2. Hirsch AT, Duval S. The global pandemic of peripheral artery disease. *The Lancet*. 2013;382(9901):1312-1314. doi:10.1016/S0140-6736(13)61576-7.

3. Brevetti G, Schiano V, Chiariello M. Endothelial dysfunction: A key to the pathophysiology and natural history of peripheral arterial disease? *Atherosclerosis*. 2008;197(1):1-11. doi:10.1016/j.atherosclerosis.2007.11.002.

4. Hirsch AT, Hartman L, Town RJ, Virnig BA. National health care costs of peripheral arterial disease in the Medicare population. *Vasc Med*. 2008;13(3):209-215. doi:10.1177/1358863X08089277.

5. Scully RE, Arnaoutakis DJ, DeBord Smith A, Semel M, Nguyen LL. Estimated annual health care expenditures in individuals with peripheral arterial disease. *J Vasc Surg*. 2018;67(2):558-567. doi:10.1016/j.jvs.2017.06.102.

6. Muller MD, Reed AB, Leuenberger UA, Sinoway LI. Physiology in Medicine: Peripheral arterial disease. *J Appl Physiol (1985)*. 2013;115(9):1219-1226. doi:10.1152/japplphysiol.00885.2013.

7. Hiatt William R., Armstrong Ehrin J., Larson Christopher J., Brass Eric P. Pathogenesis of the Limb Manifestations and Exercise Limitations in Peripheral Artery Disease. *Circulation Research*. 2015;116(9):1527-1539. doi:10.1161/CIRCRESAHA.116.303566.

8. Criqui Michael H., Aboyans Victor. Epidemiology of Peripheral Artery Disease. *Circulation Research*. 2015;116(9):1509-1526. doi:10.1161/CIRCRESAHA.116.303849.

9. Rehring TF, Sandhoff BG, Stolcpart RS, Merenich JA, Hollis HW. Atherosclerotic risk factor control in patients with peripheral arterial disease. *Journal of Vascular Surgery*. 2005;41(5):816-822. doi:10.1016/j.jvs.2005.01.047.

10. Aronow WS. Peripheral arterial disease of the lower extremities. *Arch Med Sci*. 2012;8(2):375-388. doi:10.5114/aoms.2012.28568.

11. Weintraub WS. The vascular effects of cilostazol. *Can J Cardiol*. 2006;22(Suppl B):56B-60B.

12. Thukkani Arun K., Kinlay Scott. Endovascular Intervention for Peripheral Artery Disease. *Circulation Research*. 2015;116(9):1599-1613. doi:10.1161/CIRCRESAHA.116.303503.

13. O'Donnell M, Reid J, Lau L, Hannon R, Lee B. Optimal Management of Peripheral Arterial Disease for the Non-Specialist. *Ulster Med J*. 2011;80(1):33-41.

14. Waters RE, Terjung RL, Peters KG, Annex BH. Preclinical models of human peripheral arterial occlusive disease: implications for investigation of therapeutic agents. *Journal of applied physiology*. 2004;97(2):773-780. doi:10.1152/japplphysiol.00107.2004.

15. Iyer SR, Annex BH. Therapeutic Angiogenesis for Peripheral Artery Disease. *JACC Basic Transl Sci*. 2017;2(5):503-512. doi:10.1016/j.jacbts.2017.07.012.

16. Hellingman AA, Bastiaansen AJNM, de Vries MR, Seghers L, Lijkwan MA, Löwik CW, Hamming JF, Quax PHA. Variations in Surgical Procedures for Hind Limb Ischaemia Mouse Models Result in differences in Collateral Formation. *European Journal of Vascular and Endovascular Surgery*. 2010;40(6):796-803. doi:10.1016/j.ejvs.2010.07.009.

17. Niiyama H, Huang NF, Rollins MD, Cooke JP. Murine Model of Hindlimb Ischemia. *JoVE (Journal of Visualized Experiments)*. 2009;(23):e1035. doi:10.3791/1035.

18. Hazarika Surovi, Dokun Ayotunde O., Li Yongjun, Popel Aleksander S., Kontos Christopher D., Annex Brian H. Impaired Angiogenesis After Hindlimb Ischemia in Type 2 Diabetes Mellitus. *Circulation Research*. 2007;101(9):948-956. doi:10.1161/CIRCRESAHA.107.160630.

19. Lotfi S, Patel AS, Mattock K, Egginton S, Smith A, Modarai B. Towards a more relevant hind limb model of muscle ischaemia. *Atherosclerosis*. 2013;227(1):1-8. doi:10.1016/j.atherosclerosis.2012.10.060.

20. Davis MA, Kazmi SMS, Dunn AK. Imaging depth and multiple scattering in laser speckle contrast imaging. *J Biomed Opt*. 2014;19(8). doi:10.1117/1.JBO.19.8.086001.

21. Kramer CM. Skeletal Muscle Perfusion in Peripheral Arterial Disease. *JACC Cardiovasc Imaging*. 2008;1(3):351-353. doi:10.1016/j.jcmg.2008.03.004.

22. Wei K, Jayaweera AR, Firoozan S, Linka A, Skyba DM, Kaul S. Quantification of Myocardial Blood Flow With Ultrasound-Induced Destruction of Microbubbles Administered as a Constant Venous Infusion. *Circulation*. 1998;97(5):473-483. doi:10.1161/01.CIR.97.5.473.

23. Baltgalvis KA, White K, Li W, Claypool MD, Lang W, Alcantara R, Singh BK, Friera AM, McLaughlin J, Hansen D, McCaughey K, Nguyen H, Smith IJ, Godinez G, Shaw SJ, Goff D, Singh R, Markovtsov V, Sun T-Q, Jenkins Y, Uy G, Li Y, Pan A,

Gururaja T, Lau D, Park G, Hitoshi Y, Payan DG, Kinsella TM. Exercise performance and peripheral vascular insufficiency improve with AMPK activation in high-fat diet-fed mice. *American Journal of Physiology-Heart and Circulatory Physiology*. 2014;306(8):H1128-H1145. doi:10.1152/ajpheart.00839.2013.

24. Dawson D, Vincent MA, Barrett EJ, Kaul S, Clark A, Leong-Poi H, Lindner JR. Vascular recruitment in skeletal muscle during exercise and hyperinsulinemia assessed by contrast ultrasound. *American Journal of Physiology-Endocrinology and Metabolism*. 2002;282(3):E714-E720. doi:10.1152/ajpendo.00373.2001.

25. Krix M, Weber M-A, Krakowski-Roosen H, Huttner HB, Delorme S, Kauczor H-U, Hildebrandt W. Assessment of Skeletal Muscle Perfusion Using Contrast-Enhanced Ultrasonography. *Journal of Ultrasound in Medicine*. 2005;24(4):431-441. doi:10.7863/jum.2005.24.4.431.

26. Lindner JR, Womack L, Barrett EJ, Feltman J, Price W, Harthun NL, Kaul S, Patrie JT. Limb Stress-Rest Perfusion Imaging With Contrast Ultrasound For The Assessment Of Peripheral Arterial Disease Severity. *JACC Cardiovasc Imaging*. 2008;1(3):343-350. doi:10.1016/j.jcmg.2008.04.001.

27. Kundi R, Prior SJ, Addison O, Lu M, Ryan AS, Lal BK. Contrast-Enhanced Ultrasound Reveals Exercise-Induced Perfusion Deficits in Claudicants. *J Vasc Endovasc Surg*. 2017;2(1). https://www.ncbi.nlm.nih.gov/pmc/articles/PMC5501290/. Accessed April 14, 2019.

28. Kochi T, Imai Y, Takeda A, Watanabe Y, Mori S, Tachi M, Kodama T. Characterization of the Arterial Anatomy of the Murine Hindlimb: Functional Role in the Design and Understanding of Ischemia Models. *PLOS ONE*. 2013;8(12):e84047. doi:10.1371/journal.pone.0084047.

29. Helisch Armin, Wagner Shawn, Khan Nadeem, Drinane Mary, Wolfram Swen, Heil Matthias, Ziegelhoeffer Tibor, Brandt Ulrike, Pearlman Justin D., Swartz Harold M., Schaper Wolfgang. Impact of Mouse Strain Differences in Innate Hindlimb Collateral Vasculature. *Arteriosclerosis, Thrombosis, and Vascular Biology*. 2006;26(3):520-526. doi:10.1161/01.ATV.0000202677.55012.a0.

30. Ouriel K. Peripheral arterial disease. *The Lancet*. 2001;358(9289):1257-1264. doi:10.1016/S0140-6736(01)06351-6.

31. Krishna SM, Omer SM, Golledge J. Evaluation of the clinical relevance and limitations of current pre-clinical models of peripheral artery disease. *Clinical Science*. 2016;130(3):127-150. doi:10.1042/CS20150435.

32. Cardinal TR, Hoying JB. A modified fluorescent microsphere-based approach for determining resting and hyperemic blood flows in individual murine skeletal muscles. *Vascul Pharmacol*. 2007;47(1):48-56. doi:10.1016/j.vph.2007.04.002.

33. Prinzen F. Blood flow distributions by microsphere deposition methods. *Cardiovascular Research*. 2000;45(1):13-21. doi:10.1016/S0008-6363(99)00252-7.

34. Boas DA, Dunn AK. Laser speckle contrast imaging in biomedical optics. *J Biomed Opt*. 2010;15(1). doi:10.1117/1.3285504.

35. Draijer M, Hondebrink E, van Leeuwen T, Steenbergen W. Review of laser speckle contrast techniques for visualizing tissue perfusion. *Lasers Med Sci*. 2008;24(4):639. doi:10.1007/s10103-008-0626-3.

36. Briers JD. Laser speckle contrast analysis (LASCA): a nonscanning, full-field technique for monitoring capillary blood flow. *J Biomed Opt*. 1996;1(2):174. doi:10.1117/12.231359.

37. Senarathna J, Rege A, Li N, Thakor NV. Laser Speckle Contrast Imaging: Theory, Instrumentation and Applications. *IEEE Reviews in Biomedical Engineering*. 2013;6:99-110. doi:10.1109/RBME.2013.2243140.

38. Schinkel AFL, Kaspar M, Staub D. Contrast-enhanced ultrasound: clinical applications in patients with atherosclerosis. *Int J Cardiovasc Imaging*. 2016;32(1):35-48. doi:10.1007/s10554-015-0713-z.

39. Halpern EJ. Contrast-Enhanced Ultrasound Imaging of Prostate Cancer. *Rev Urol*. 2006;8(Suppl 1):S29-S37.

40. Sullivan JC, Wang B, Boesen EI, D'Angelo G, Pollock JS, Pollock DM. Novel use of ultrasound to examine regional blood flow in the mouse kidney. *American Journal of Physiology-Renal Physiology*. 2009;297(1):F228-F235. doi:10.1152/ajprenal.00016.2009.

41. Baron David M., Clerte Maeva, Brouckaert Peter, Raher Michael J., Flynn Aidan W., Zhang Haihua, Carter Edward A., Picard Michael H., Bloch Kenneth D., Buys Emmanuel S., Scherrer-Crosbie Marielle. In Vivo Noninvasive Characterization of Brown Adipose Tissue Blood Flow by Contrast Ultrasound in Mice. *Circulation: Cardiovascular Imaging*. 2012;5(5):652-659. doi:10.1161/CIRCIMAGING.112.975607.

42. French BA, Li Y, Klibanov AL, Yang Z, Hossack JA. 3D perfusion mapping in post-infarct mice using myocardial contrast echocardiography. *Ultrasound in Medicine & Biology*. 2006;32(6):805-815. doi:10.1016/j.ultrasmedbio.2006.03.002.

43. Pysz MA, Foygel K, Panje CM, Needles A, Tian L, Willmann JK. Assessment and Monitoring Tumor Vascularity With Contrast-Enhanced Ultrasound Maximum Intensity Persistence Imaging. *Invest Radiol*. 2011;46(3):187-195. doi:10.1097/RLI.0b013e3181f9202d.

44. Rissanen TT, Korpisalo P, Karvinen H, Liimatainen T, Laidinen S, Gröhn OH, Ylä-Herttuala S. High-Resolution Ultrasound Perfusion Imaging of Therapeutic

Angiogenesis. *JACC: Cardiovascular Imaging*. 2008;1(1):83-91. doi:10.1016/j.jcmg.2007.10.009.

45. Karvinen H, Pasanen E, Rissanen TT, Korpisalo P, Vähäkangas E, Jazwa A, Giacca M, Ylä-Herttuala S. Long-term VEGF-A expression promotes aberrant angiogenesis and fibrosis in skeletal muscle. *Gene Therapy*. 2011;18(12):1166-1172. doi:10.1038/gt.2011.66.

46. Kuliszewski MA, Kobulnik J, Lindner JR, Stewart DJ, Leong-Poi H. Vascular Gene Transfer of SDF-1 Promotes Endothelial Progenitor Cell Engraftment and Enhances Angiogenesis in Ischemic Muscle. *Molecular Therapy*. 2011;19(5):895-902. doi:10.1038/mt.2011.18.

47. Laser Speckle Contrast Analysis | Perimed. https://www.perimed-instruments.com/laser-speckle-contrast-analysis/. Accessed June 8, 2019.

48. Briers D, Duncan DD, Hirst ER, Kirkpatrick SJ, Larsson M, Steenbergen W, Stromberg T, Thompson OB. Laser speckle contrast imaging: theoretical and practical limitations. *JBO*. 2013;18(6):066018. doi:10.1117/1.JBO.18.6.066018.

49. Wang Y, Marshall KL, Baba Y, Lumpkin EA, Gerling GJ. Compressive Viscoelasticity of Freshly Excised Mouse Skin Is Dependent on Specimen Thickness, Strain Level and Rate. *PLOS ONE*. 2015;10(3):e0120897. doi:10.1371/journal.pone.0120897.

50. Calabro K, Curtis A, Galarneau J-R, Krucker T, Bigio IJ. Gender variations in the optical properties of skin in murine animal models. *J Biomed Opt*. 2011;16(1):011008. doi:10.1117/1.3525565.

51. Fleischmann D, Hallett RL, Rubin GD. CT Angiography of Peripheral Arterial Disease. *Journal of Vascular and Interventional Radiology*. 2006;17(1):3-26. doi:10.1097/01.RVI.0000191361.02857.DE.

52. Tirziu D, Moodie KL, Zhuang ZW, Singer K, Helisch A, Dunn JF, Li W, Singh J, Simons M. Delayed Arteriogenesis in Hypercholesterolemic Mice. *Circulation*. 2005;112(16):2501-2509. doi:10.1161/CIRCULATIONAHA.105.542829.

53. Frinking PJA, Bouakaz A, Kirkhorn J, Ten Cate FJ, de Jong N. Ultrasound contrast imaging: current and new potential methods. *Ultrasound in Medicine & Biology*. 2000;26(6):965-975. doi:10.1016/S0301-5629(00)00229-5.

54. Phillips PJ. Contrast pulse sequences (CPS): imaging nonlinear microbubbles. In: *2001 IEEE Ultrasonics Symposium. Proceedings. An International Symposium (Cat. No.01CH37263)*. Vol 2. ; 2001:1739-1745 vol.2. doi:10.1109/ULTSYM.2001.992057.

55. Unnikrishnan S, Du Z, Diakova GB, Klibanov AL. Formation of Microbubbles for Targeted Ultrasound Contrast Imaging: Practical Translation Considerations. *Langmuir*. December 2018. doi:10.1021/acs.langmuir.8b03551.

56. Serrat MA. Measuring bone blood supply in mice using fluorescent microspheres. *Nature Protocols*. 2009;4(12):1749-1758. doi:10.1038/nprot.2009.190.

57. Buckberg GD, Luck JC, Payne DB, Hoffman JI, Archie JP, Fixler DE. Some sources of error in measuring regional blood flow with radioactive microspheres. *Journal of Applied Physiology*. 1971;31(4):598-604. doi:10.1152/jappl.1971.31.4.598.

58. Jädert C, Petersson J, Massena S, Ahl D, Grapensparr L, Holm L, Lundberg JO, Phillipson M. Decreased leukocyte recruitment by inorganic nitrate and nitrite in microvascular inflammation and NSAID-induced intestinal injury. *Free Radical Biology and Medicine*. 2012;52(3):683-692. doi:10.1016/j.freeradbiomed.2011.11.018.

59. Susaki EA, Tainaka K, Perrin D, Yukinaga H, Kuno A, Ueda HR. Advanced CUBIC protocols for whole-brain and whole-body clearing and imaging. *Nature Protocols*. 2015;10(11):1709-1727. doi:10.1038/nprot.2015.085.

60. Ning B, Kennedy MJ, Dixon AJ, Sun N, Cao R, Soetikno BT, Chen R, Zhou Q, Shung KK, Hossack JA, Hu S. Simultaneous photoacoustic microscopy of microvascular anatomy, oxygen saturation, and blood flow. *Opt Lett, OL*. 2015;40(6):910-913. doi:10.1364/OL.40.000910.

61. Mayrovitz HN, Larsen PB. Pulsatile blood flow asymmetry in paired human legs. *Clinical Physiology*. 1996;16(5):495-505. doi:10.1111/j.1475-097X.1996.tb01015.x.

62. Marcinkevics Z, Lukstina Z, Rubins U, Grabovskis A, Aivars J-I. Bilateral difference of superficial and deep femoral artery haemodynamic and anatomical parameters. *Artery Research*. 2013;7(3):201-210. doi:10.1016/j.artres.2013.09.001.

63. Arpino John-Michael, Nong Zengxuan, Li Fuyan, Yin Hao, Ghonaim Nour, Milkovich Stephanie, Balint Brittany, O'Neil Caroline, Fraser Graham M., Goldman Daniel, Ellis Christopher G., Pickering J. Geoffrey. Four-Dimensional Microvascular Analysis Reveals That Regenerative Angiogenesis in Ischemic Muscle Produces a Flawed Microcirculation. *Circulation Research*. 2017;120(9):1453-1465. doi:10.1161/CIRCRESAHA.116.310535.

64. Stabile Eugenio, Burnett Mary Susan, Watkins Craig, Kinnaird Timothy, Bachis Alessia, la Sala Andrea, Miller Jonathan M., Shou Matie, Epstein Stephen E., Fuchs Shmuel. Impaired Arteriogenic Response to Acute Hindlimb Ischemia in CD4-Knockout Mice. *Circulation*. 2003;108(2):205-210. doi:10.1161/01.CIR.0000079225.50817.71.

65. Couffinhal T, Silver M, Zheng LP, Kearney M, Witzenbichler B, Isner JM. Mouse model of angiogenesis. *Am J Pathol*. 1998;152(6):1667-1679.

66. Collins RL. When Left-Handed Mice Live in Right-Handed Worlds. *Science, New Series*. 1975;187(4172):181-184.

67. Brenes RA, Jadlowiec CC, Bear M, Hashim P, Protack CD, Li X, Lv W, Collins MJ, Dardik A. Toward a mouse model of hind limb ischemia to test therapeutic angiogenesis. *Journal of Vascular Surgery*. 2012;56(6):1669-1679. doi:10.1016/j.jvs.2012.04.067.

68. Lian Q, Zhang Y, Zhang J, Zhang H, Wu X, Zhang Y, Lam FF-Y, Kang S, Xia JC, Lai W, Au KTP, Chow YY, Siu CD, Lee C, Tse H. Functional mesenchymal stem cells derived from human induced pluripotent stem cells attenuate limb ischemia in mice. *Circulation*. 2010;121(9):1113-1123. doi:10.1161/CIRCULATIONAHA.109.898312.

69. Landázuri N, Joseph G, Guldberg RE, Taylor WR. Growth and regression of vasculature in healthy and diabetic mice after hindlimb ischemia. *Am J Physiol Regul Integr Comp Physiol*. 2012;303(1):R48-R56. doi:10.1152/ajpregu.00002.2012.

70. Stoyioglou A, Jaff MR. Medical Treatment of Peripheral Arterial Disease: A Comprehensive Review. *Journal of Vascular and Interventional Radiology*. 2004;15(11):1197-1207. doi:10.1097/01.RVI.0000137978.15352.C6.

71. Bajwa Adnan, Wesolowski Roman, Patel Ashish, Saha Prakash, Ludwinski Francesca, Smith Alberto, Nagel Eike, Modarai Bijan. Assessment of Tissue Perfusion in the Lower Limb. *Circulation: Cardiovascular Imaging*. 2014;7(5):836-843. doi:10.1161/CIRCIMAGING.114.002123.

72. Nguyen T, Davidson BP. Contrast Enhanced Ultrasound Perfusion Imaging in Skeletal Muscle. *Journal of Cardiovascular Imaging*. 2019;27. doi:10.4250/jcvi.2019.27.e31.

73. Davidson BP, Belcik JT, Landry G, Linden J, Lindner JR. EXERCISE VERSUS VASODILATOR STRESS LIMB PERFUSION IMAGING FOR THE ASSESSMENT OF PERIPHERAL ARTERY DISEASE. *Echocardiography*. 2017;34(8):1187-1194. doi:10.1111/echo.13601.

74. Shuoqi Ye SY, Junyu Yang JY, Jianzhong Xi JX, Qiushi Ren QR, Changhui Li CL. Studying murine hindlimb ischemia by photoacoustic microscopy. *Chin Opt Lett*. 2012;10(12):121701-121704. doi:10.3788/COL201210.121701.

75. Annex BH. Therapeutic angiogenesis for critical limb ischaemia. *Nature Reviews Cardiology*. 2013;10(7):387-396. doi:10.1038/nrcardio.2013.70.

76. McDermott MM, Greenland P, Liu K, Guralnik JM, Criqui MH, Dolan NC, Chan C, Celic L, Pearce WH, Schneider JR, Sharma L, Clark E, Gibson D, Martin GJ. Leg Symptoms in Peripheral Arterial Disease: Associated Clinical Characteristics and Functional Impairment. *JAMA*. 2001;286(13):1599-1606. doi:10.1001/jama.286.13.1599.

77. Morcos R, Louka B, Tseng A, Misra S, McBane R, Esser H, Shamoun F. The Evolving Treatment of Peripheral Arterial Disease through Guideline-Directed Recommendations. *Journal of Clinical Medicine*. 2018;7(1):9. doi:10.3390/jcm7010009.

78. Lin J, Phillips E, Riggins T, Sangha G, Chakraborty S, Lee J, Lycke R, Hernandez C, Soepriatna A, Thorne B, Yrineo A, Goergen C. Imaging of Small Animal Peripheral Artery Disease Models: Recent Advancements and Translational Potential. *IJMS*. 2015;16(12):11131-11177. doi:10.3390/ijms160511131.

79. Schaad L, Hlushchuk R, Barré S, Gianni-Barrera R, Haberthür D, Banfi A, Djonov V. Correlative Imaging of the Murine Hind Limb Vasculature and Muscle Tissue by MicroCT and Light Microscopy. *Scientific Reports*. 2017;7:41842. doi:10.1038/srep41842.

80. Chalothorn D, Faber JE. Strain-dependent variation in collateral circulatory function in mouse hindlimb. *Physiological Genomics*. 2010;42(3):469-479. doi:10.1152/physiolgenomics.00070.2010.

81. McClung JM, McCord TJ, Keum S, Johnson S, Annex BH, Marchuk DA, Kontos CD. Skeletal Muscle–Specific Genetic Determinants Contribute to the Differential Strain-Dependent Effects of Hindlimb Ischemia in Mice. *The American Journal of Pathology*. 2012;180(5):2156-2169. doi:10.1016/j.ajpath.2012.01.032.

82. Treat-Jacobson D, Halverson SL, Ratchford A, Regensteiner JG, Lindquist R, Hirsch AT. A Patient-Derived Perspective of Health-Related Quality of Life With Peripheral Arterial Disease. *J Nursing Scholarship*. 2002;34(1):55-60. doi:10.1111/j.1547-5069.2002.00055.x.

83. Belch JJF, Topol EJ, Agnelli G, Bertrand M, Califf RM, Clement DL, Creager MA, Easton JD, Gavin JR, Greenland P, Hankey G, Hanrath P, Hirsch AT, Meyer J, Smith SC, Sullivan F, Weber MA. Critical Issues in Peripheral Arterial Disease Detection and Management: A Call to Action. *Arch Intern Med*. 2003;163(8):884-892. doi:10.1001/archinte.163.8.884.

84. Hiatt WR, Wolfel EE, Meier RH, Regensteiner JG. Superiority of treadmill walking exercise versus strength training for patients with peripheral arterial disease. Implications for the mechanism of the training response. *Circulation*. 1994;90(4):1866-1874. doi:10.1161/01.CIR.90.4.1866.

85. Makris GC, Lattimer CR, Lavida A, Geroulakos G. Availability of Supervised Exercise Programs and the Role of Structured Home-based Exercise in Peripheral

Arterial Disease. *European Journal of Vascular and Endovascular Surgery*. 2012;44(6):569-575. doi:10.1016/j.ejvs.2012.09.009.

86. Murphy TP, Cutlip DE, Regensteiner JG, Mohler ER, Cohen DJ, Reynolds MR, Massaro JM, Lewis BA, Cerezo J, Oldenburg NC, Thum CC, Jaff MR, Comerota AJ, Steffes MW, Abrahamsen IH, Goldberg S, Hirsch AT. Supervised Exercise, Stent Revascularization, or Medical Therapy for Claudication Due to Aortoiliac Peripheral Artery Disease. *Journal of the American College of Cardiology*. 2015;65(10):999-1009. doi:10.1016/j.jacc.2014.12.043.

87. Abaraogu U, Ezenwankwo E, Dall P, Tew G, Stuart W, Brittenden J, Seenan C. Barriers and enablers to walking in individuals with intermittent claudication: A systematic review to conceptualize a relevant and patient-centered program. *PLOS ONE*. 2018;13(7):e0201095. doi:10.1371/journal.pone.0201095.

88. Pande RL, Hiatt WR, Zhang P, Hittel N, Creager MA. A pooled analysis of the durability and predictors of treatment response of cilostazol in patients with intermittent claudication. *Vasc Med*. 2010;15(3):181-188. doi:10.1177/1358863X10361545.

89. Vartanian Shant M., Conte Michael S. Surgical Intervention for Peripheral Arterial Disease. *Circulation Research*. 2015;116(9):1614-1628. doi:10.1161/CIRCRESAHA.116.303504.

90. Secemsky EA, Schermerhorn M, Carroll BJ, Kennedy KF, Shen C, Valsdottir LR, Landon B, Yeh RW. Readmissions After Revascularization Procedures for Peripheral Arterial Disease: A Nationwide Cohort Study. *Ann Intern Med*. 2018;168(2):93. doi:10.7326/M17-1058.

91. Ramkumar Niveditta, Martinez-Camblor Pablo, Columbo Jesse A., Osborne Nicholas H., Goodney Philip P., O'Malley A. James. Adverse Events After Atherectomy: Analyzing Long-Term Outcomes of Endovascular Lower Extremity Revascularization Techniques. *Journal of the American Heart Association*. 2019;8(12):e012081. doi:10.1161/JAHA.119.012081.

92. Grochot-Przeczek A, Dulak J, Jozkowicz A. Therapeutic angiogenesis for revascularization in peripheral artery disease. *Gene*. 2013;525(2):220-228. doi:10.1016/j.gene.2013.03.097.

93. Shimamura M, Nakagami H, Taniyama Y, Morishita R. Gene therapy for peripheral arterial disease. *Expert Opinion on Biological Therapy*. 2014;14(8):1175-1184. doi:10.1517/14712598.2014.912272.

94. Fasanaro P, Greco S, Ivan M, Capogrossi MC, Martelli F. microRNA: Emerging therapeutic targets in acute ischemic diseases. *Pharmacology & Therapeutics*. 2010;125(1):92-104. doi:10.1016/j.pharmthera.2009.10.003.

95. Koutakis P, Ismaeel A, Farmer P, Purcell S, Smith RS, Eidson JL, Bohannon WT. Oxidative stress and antioxidant treatment in patients with peripheral artery disease. *Physiol Rep*. 2018;6(7). doi:10.14814/phy2.13650.

96. New horizons in the treatment of lower extremity arterial disease. https://www.escardio.org/Journals/E-Journal-of-Cardiology-Practice/Volume-16/New-horizons-in-the-treatment-of-lower-extremity-arterial-disease. Accessed June 10, 2019.

97. Yang Z, Laubach VE, French BA, Kron IL. Acute hyperglycemia enhances oxidative stress and exacerbates myocardial infarction by activating NADPH oxidase during reperfusion. *J Thorac Cardiovasc Surg*. 2009;137(3):723-729. doi:10.1016/j.jtcvs.2008.08.056.

98. Yadav V, Marracci GH, Munar MY, Cherala G, Stuber LE, Alvarez L, Shinto L, Koop DR, Bourdette DN. Pharmacokinetic study of lipoic acid in multiple sclerosis: Comparing mice and human pharmacokinetic parameters. *Mult Scler*. 2010;16(4):387-397. doi:10.1177/1352458509359722.

99. Fogel DB. Factors associated with clinical trials that fail and opportunities for improving the likelihood of success: A review. *Contemp Clin Trials Commun*. 2018;11:156-164. doi:10.1016/j.conctc.2018.08.001.

100. Scholz D, Ziegelhoeffer T, Helisch A, Wagner S, Friedrich C, Podzuweit T, Schaper W. Contribution of Arteriogenesis and Angiogenesis to Postocclusive Hindlimb Perfusion in Mice. *Journal of Molecular and Cellular Cardiology*. 2002;34(7):775-787. doi:10.1006/jmcc.2002.2013.

101. Wang Tao, Cunningham Alexis, Dokun Ayotunde O., Hazarika Surovi, Houston Kevin, Chen Lingdan, Lye R. John, Spolski Rosanne, Leonard Warren J., Annex Brian H. Loss of Interleukin-21 Receptor Activation in Hypoxic Endothelial Cells Impairs Perfusion Recovery After Hindlimb Ischemia. *Arteriosclerosis, Thrombosis, and Vascular Biology*. 2015;35(5):1218-1225. doi:10.1161/ATVBAHA.115.305476.

102. Nossent A. Yaël, Bastiaansen Antonius J. N. M., Peters Erna A. B., de Vries Margreet R., Aref Zeen, Welten Sabine M. J., de Jager Saskia C. A., van der Pouw Kraan Tineke C. T. M., Quax Paul H. A. CCR7-CCL19/CCL21 Axis is Essential for Effective Arteriogenesis in a Murine Model of Hindlimb Ischemia. *Journal of the American Heart Association*. 6(3):e005281. doi:10.1161/JAHA.116.005281.

103. la Sala A, Pontecorvo L, Agresta A, Rosano G, Stabile E. Regulation of collateral blood vessel development by the innate and adaptive immune system. *Trends in Molecular Medicine*. 2012;18(8):494-501. doi:10.1016/j.molmed.2012.06.007.

104. Hallenbeck JM, Hansson GK, Becker KJ. Immunology of ischemic vascular disease: plaque to attack. *Trends in Immunology*. 2005;26(10):550-556. doi:10.1016/j.it.2005.08.007.

105. Ouma GO, Jonas RA, Usman MHU, Mohler ER. Targets and delivery methods for therapeutic angiogenesis in peripheral artery disease. *Vasc Med*. 2012;17(3):174-192. doi:10.1177/1358863X12438270.

106. Agyare E, Kandimalla K. Delivery of Polymeric Nanoparticles to Target Vascular Diseases. *J Biomol Res Ther*. 2014;3(1). https://www.ncbi.nlm.nih.gov/pmc/articles/PMC4460796/. Accessed June 11, 2019.

107. Roselli RJ, Diller KR. *Biotransport: Principles and Applications*. New York: Springer-Verlag; 2011. https://www.springer.com/us/book/9781441981189. Accessed June 7, 2019.